Diagnostics in Liver Diseases

8 Radiological diagnostics

8 Radiological diagnostics

A definite diagnosis is often not obtained in liver disease despite the combined use of the **mainstays of diagnostics:** (*1.*) *clinical findings*, (*2.*) *laboratory examination data*, and (*3.*) *ultrasonography.* Possibly, even (*4.*) *morphological analysis* has been unproductive or was not indicated at all. This raises the question of using special radiological and nuclear medical examination techniques. • Diagnostic problems may arise, especially with regard to the following **issues:**

- Identification of intrahepatic foci
- Clarification of the benignancy or malignancy of focal liver lesions
- Differentiation of vascular-related liver diseases
- Detection of alterations regarding the bile ducts
- Differential diagnosis of mechanical jaundice
- Assessment of portal hypertension
- Extent of collateral vessels
- Unclarified diffuse alterations of the liver
- Control following liver trauma
- Staging of malignant tumours
- Checking indications for surgical intervention
- Examination before and follow-up after LT

Different **radiological procedures** are available for clarifying these diagnostic issues. (s. tab. 8.1)

1. Computer tomography (CT)
2. Magnetic resonance imaging (MRI)
3. Arteriography
4. Portography
5. Phlebography
6. Cholangiography

Tab. 8.1: Radiological procedures used in the diagnosis of hepatobiliary diseases

These various imaging techniques (s. tab. 8.1) – as well as some nuclear medicine-based methods (*see chapter 9*) – enable key features of benign and malignant tumours to be recognized, including (*1.*) vascularity, (*2.*) internal structure, (*3.*) hepatocyte functions, (*4.*) biliary tract, (*5.*) bile secretion, (*6.*) calcification, and (*7.*) Kupffer cell activity.

1 Computer tomography

► Tomography was developed by A.E.M. Bocage and registered as a French patent in the same year. It was further developed in the form of transversal (and axial) tomography by H. Vieten (1936) and registered as a German patent. A research team headed by A. Gebauer presented a device for use in clinical practice in 1945.

► The **introduction** of computer tomography (CT) into medicine by G. N. Hounsfield in 1971 (skull CT) and as computerized transverse axial scanning (tomography) in 1973 was a revolutionary event comparable with the discovery of X-rays by W. C. Röntgen in 1895. (15) • As early as 1975, the first normal CT scan of the upper abdomen was reported (R. J. Alfidi et al.) (1), and in the same year, the first pathological findings from abdominal diseases (relating to the liver) were also presented (D. Schellinger et al., 1975). (38)

1.1 Principle

In computer tomography, the attenuations of many finely focused X-rays are measured by detectors and converted to electrical signals. These values are transmitted to a computer. Subsequently, the absorption value of each image point is calculated and displayed in a complex digital image. The transmission of X-rays through the body occurs in the form of fan beams and is recorded by a rotating detector fan (3rd CT generation). The 4th CT generation features a static detector crown, spanning 360 degrees, around which the X-ray source continually rotates. (9) • More advanced spiral CT facilitates spiral scanning, permitting continuous imaging of the analyzed area while the patient holds his/her breath. This provides accurate anatomical data without respiratory artefacts and with optimum exploitation of the CM bolus. (3, 5, 6, 10, 12)

In contrast to ultrasonography, which is based on the recording and imaging of the reflection of sound waves between tissues with varying acoustic impedance, the radiological signal is produced by **differences in absorption.** • With the **radiation doses** used (100–140 kv), the absorbed dose of energy corresponds to 0.013 Gy (1.3 rad) per tomographical slice. By using many finely focused X-rays, the dose is largely restricted to the body layer to be imaged. Therefore, only a relatively low scatter of radiation has to be taken into consideration. The radiation exposure of a CT scan is comparable to that of a plain radiograph of the abdomen.

With consecutive tomograms, the thickness of each section of the body is 5-8-10 (–12) mm. In individual cases, additional thin-section tomograms of 1 mm can be obtained. Resolution is 1 × 2 mm in the hepatic area, with an accuracy in attenuation values of up to 0.5%. In this way, the values for a particular cross-section and their spatial distribution are visualized in a scan. This results in blur-free, anatomically precise imaging of a layer of the body in an axial plane. CT scans provide satisfactory information if an object diameter of 1.5 to 3.0 mm is resolved with a density gradient of 0.5% to the surrounding area at an integral dose of 10 mGy.

1.2 Hounsfield units

The attenuation values are given in Hounsfield units (HU), the density scale ranging from –1,000 (= air) through 0 (= water) to +1,000 (= bone). These 2,000 shades of brightness are recorded by the computer, but are not perceived by the human eye. Due to the tech-

nical possibility of choosing only a small part of the Hounsfield scale and shifting it within an organ section, smaller differences in density can be more easily detected. Thus within certain limits, CT is indeed able to provide information about the kind of lesion involved. The special value of CT lies in the possibility of determining the density of various tissues, e.g. the structure of fatty tissue is identifiable. This option helps with the differential diagnosis of space-occupying processes (benign vs. malignant). There may be slight fluctuations in the normal Hounsfield units caused by *small vessels* included in the measuring volume. • The terms **hypodense, isodense** and **hyperdense** are used to describe pathological changes. (s. p. 132)

1.3 Contrast media

(*1*.) A major improvement in the diagnostic power from **native CT** is achieved by the use of contrast media (CM) (1.0−1.5 ml/kg BW; 1−5 ml/sec), transported via the kidney or in the bile. The CM is administered as i.v. infusion using programmable infusiomates or in the form of i.v. or intra-arterial bolus-triggering. With the conventional CT apparatus (which has a short scanning period of 0.7−5.0 seconds), i.v. administration of a CM bolus (if necessary, with additional i.v. infusion of CM) has proved most effective with regard to the subsequent rapid imaging (4−8 pictures during the first minute) of **dynamic-sequential CT.** This provides detailed assessment of CM dispersion in the intravascular and extravascular areas. (25) The differences in density between the various organs and between the normal liver parenchyma and pathological tissue structures are markedly accentuated. Furthermore, the arterial phase, enhancement of the parenchyma and the phase of venous drainage are recorded simultaneously. • The value of **cine CT** with extremely short scanning periods (7 pictures per second) has not yet been defined with respect to liver diagnostics.

(*2*.) Application of **CT arteriography** (CTA) through the hepatic artery or **CT arterioportography** (CTAP) corresponding to indirect splenoportography (i.e. via the superior mesenteric artery or splenic artery) is considered to be the most efficient procedure in the diagnosis of focal liver lesions. However, it has the disadvantage of being an invasive method. Exact indications (above all for preoperative use) have been defined. • *Modern **spiral CT** (SCTA or SCTAP) with i.v. injection of contrast medium facilitates excellent angiographic tissue reconstruction on an outpatient basis.* (6) • The development of **multidetector-row CT** (MDCT) has improved liver imaging considerably. With 40−60 row-scanners, true isotropic imaging with a z-axis resolution of 0.3−0.6 mm has become possible. (39)

1.4 Normal liver

The normal liver is characterized by smooth contours and a homogeneous density of 1.068 ± 0.005 g/cm^3. The absorption values are 60 ± 6 HU (or 64 ± 5 HU). Major vessels are delineated as hypodense areas with values of 40−45 HU. The bile ducts near the hilus are occasionally recognized by their hypodensity (5−15 HU); imaging is improved by using a biliary contrast material. CT permits good visualization of the gall bladder. The density of a normal liver is either the same as or up to 8 HU higher than that of the spleen. In some cases, the segments can be delineated.

Volumetry: Using CT, it is possible to determine the size, shape and volume of the liver with considerable accuracy. Hepatic volumetry can be performed with high-level reliability (deviation ± 5−10%). (48)

Falciform ligament: Reduction in the density values in the area of the falciform ligament is explained in the literature by fat deposition. (s. fig. 8.1) • **In more than 6,000 laparoscopies, I have never observed any fat deposition at the areas of attachment of the falciform ligament** (neither in the liver nor at the abdominal wall) or on the transparent ligament itself. (s. fig. 16.4!) • I did, however, frequently find mesenteric fatty tissue along the *round ligament*. In addition, **intrahepatic fat deposits under the falciform ligament are not known either to the anatomist or the pathologist**. • This finding is probably the round ligament, which is occasionally rich in fat, or regional (pathological?) fatty degeneration, as shown in figures 8.3 and 8.4. (s. p. 136)

► *Up to now, such (oval) fat deposition has been interpreted by the radiologist as being a falciform ligament (s. fig. 8.1) − this viewpoint must now be reconsidered. It should in any case be noted that the falciform ligament is totally devoid of fat!*

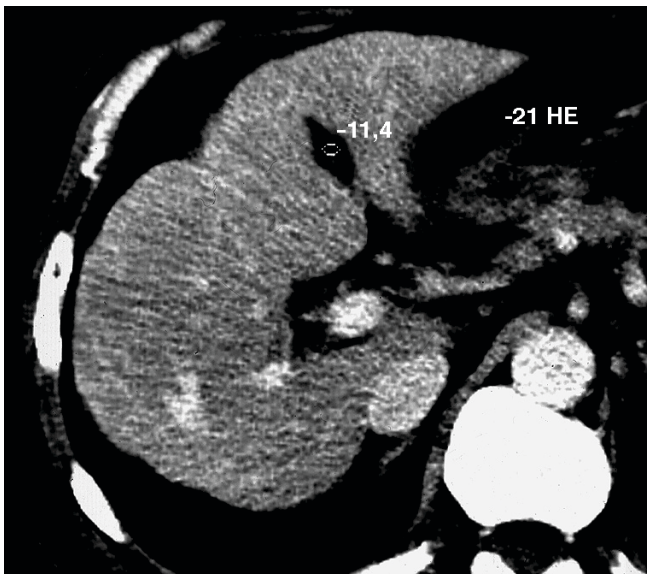

Fig. 8.1: Frequently recorded reduction in density in the area of the falciform ligament (here: 11.4 HU) resembling "fatty tissue" (possibly a round ligament?) (s. p. 136)

1.5 Contraindications

Contraindications include (*1*.) pregnancy, especially in the early stages, (*2*.) known contrast-medium intolerance (restricted to native CT), and (*3*.) renal insufficiency (in which only native CT may be used). With creatinine levels of >1.5 mg/dl, the administration of contrast material is only advisable after consulting an experienced nephrologist. (*4*.) In existing hyperthyreosis

(latent or manifest), the thyroid gland must be blocked with sodium perchlorate and even treated with carbimazole if necessary − because of the application of a CM which contains iodine (ca. 300 mg/ml). • A *relative contraindication* applies to diabetics treated with the oral antidiabetic metformin hydrochloride, as this compound competes with the CM in the kidney for elimination. The drug should be discontinued two days prior to the administration of the contrast medium.

1.6 Indications

The indication for the use of CT is only given after a careful (and as far as possible repeated) ultrasonographic examination. Due to the considerable amount of technical equipment required and the high costs involved as well as the radiation exposure associated with this method, CT is not a routine examination procedure. Clinical indications should be assessed thoroughly and must in themselves be justified. (9) (s. tab. 8.2)

1. Primary liver tumours
   - primary liver cell carcinoma (5, 11, 18, 23, 28, 30, 31)
   - haemangiopericytoma, -endothelioma
   - cholangiocarcinoma (55)
   - cystadenocarcinoma (4)
2. Secondary liver tumours
   - metastases (22, 39, 50, 53, 57)
3. Benign liver tumours
   - cysts (51)
   - abscesses
   - adenoma, FNH (2, 23, 24, 26, 34, 37, 42, 52)
   - haemangioma (17, 32, 35, 40, 54)
   - echinococcus (8)
   - tuberculosis (19, 21)
   - lipoma
4. Parenchymal disorders (29)
   - focal fatty infiltration (13, 36, 40, 45, 56)
   - cirrhosis (49)
   - haemochromatosis (20, 29)
   - primary sclerosing cholangitis (7)
5. Mechanical jaundice (47)
6. Condition following liver trauma (33, 41)
   - haematoma
   - rupture
7. Caroli's syndrome (16, 44)
8. Prior to and after liver transplantation (43)
9. Fasciola hepatica (14)
10. Unknown ascites
11. Splenomegaly
12. Budd-Chiari syndrome (27)
13. Portal vein system (46)
14. Interventional measures
    - punctures, drainage tubes
    - chemoembolization

Tab. 8.2: Indications for computer tomography in hepatobiliary diseases (with some references)

1.7 Diffuse liver diseases

1.7.1 Fatty liver

In correlation with fatty infiltration, the fatty liver shows a *diffuse reduction in density* with decreased Hounsfield units. The fatty liver appears much darker than the spleen (= *grey liver*). Hepatomegaly with smooth contours is visible. The parenchyma is isodense or hypodense compared with the vessels and bile ducts, which is why (depending on the degree of fatty infiltration) there is a reversal of density (= *negative scan*). A linear correlation exists between the extent of the fatty infiltration and the decrease in the density recorded. An increase in the relative fat content by 10% leads to a reduction in density of 17(−20) HU. • With fatty degeneration of about 80%, the density is decreased to approx. −50 HU. CT may be useful in controlling the course of a fatty liver, a scan through the middle of the liver being sufficient for this purpose. Dif-

Fig. 8.2: Pronounced, toxic fatty liver following cytostatic chemotherapy with recorded values of between −9.9 and −1.1 HU. The liver is homogeneously dark (compared to the bright spleen). The vessels appear brighter (values of between +40 and +50 HU)

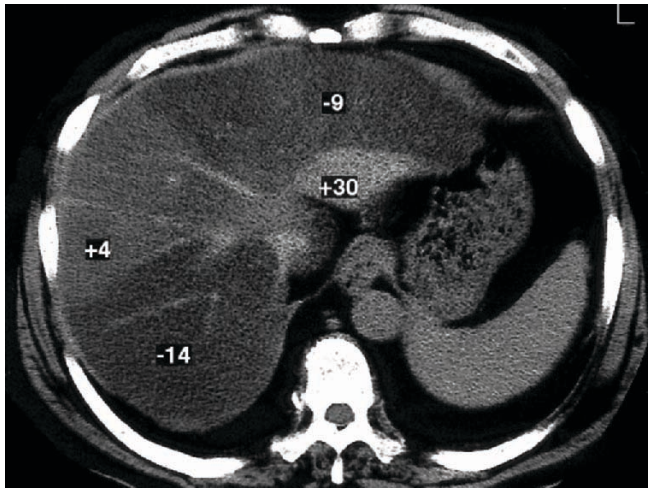

Fig. 8.3: Pronounced focal (regional) fatty degeneration of the liver of varying intensity: both visual and confirmed by Hounsfield units (−14, −9, +4, +30). Native CT, normal value +65 HU

ferentiation between hepatocellular *fatty infiltration* and *fatty liver* is not feasible with CT. The detection rate for diagnosing a fatty liver by means of CT is 85−95%. (s. fig. 8.2) • Besides being diffuse and homogeneous, the fatty liver may also exhibit regional (lobular or segmental) *focal fatty infiltration* of varying degrees. (s. figs. 8.3, 8.4) (cf. figs. 6.12, 6.13) Occasionally, focal infiltration is only barely, or not at all, distinguishable from a malignant tumour. Here MRI is an important additional procedure. (13, 36, 40, 45, 56) *(see chapter 31.3)*

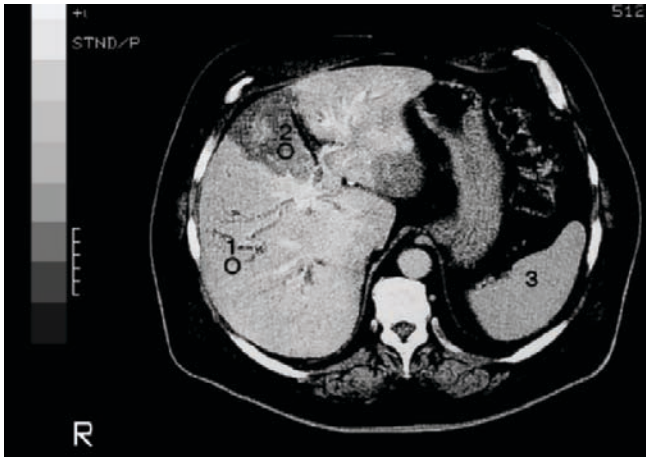

Fig. 8.4: Segmental fatty degeneration of the liver (2 = 37.3 HU) following application of CM compared to liver parenchyma of normal density (1 = 68.5 HU), and the spleen (3)

1.7.2 Liver cirrhosis

As a rule, liver cirrhosis exhibits absorption values which are no different from those of a normal liver. Advanced stages show an enlargement of the caudate lobe and possibly also of the left lobe as well as alterations in form or shrinkage of the right lobe (or both lobes) with fine to coarse nodular irregularities on the surface. In some cases, an increase in density of up to 60−70 HU is verifiable. Usually, splenomegaly and further signs of portal hypertension are present. • Hypodense foci may indicate HCC and should be examined with the aid of contrast medium or MRI. (7, 29, 46, 49)

1.7.3 Haemochromatosis

Haemochromatosis leads to an increase in the density of the liver parenchyma, which correlates with the accumulation of iron. CT scans reveal a remarkably dense and bright liver parenchyma with density values of up to +140 HU (so-called *"white liver"*). The deposition of 1 g iron results in a rise in density of 1 HU. (20) CT densitometry clearly facilitates effective control of therapeutic success in this storage disease. It is not possible, however, to differentiate pronounced secondary haemosiderosis. • *Hyperdense values* are also found in long-term **gold therapy,** in **glycogen thesaurismosis** and **M. Wilson**, or in chronic **arsenic poisoning.**

1.8 Focal liver lesions

Even by means of computer tomography (like ultrasonography), a definitive distinction cannot be made between primary and secondary or benign and malignant liver tumours, except in the case of liver lipoma. However, differentiation is greatly improved by using contrast medium and CT angiography. Radiomorphological identification of focal lesions with a diameter of < 0.3−0.8 cm is not (yet) possible, even with the aid of more sophisticated appliances: geometric resolution and density resolution have their limits. The density analysis of focal findings will thus only yield reliable information if the diameter of the focal lesion is within the range of the twofold thickness of the section plane used. Compared to liver parenchyma, most focal lesions are hypodense. *Hyperdense values* (see above) are encountered with calcifications and occasionally also with fresh bleeding and scar tissue. (2, 12, 18, 23)

The **sensitivity** of CT for the confirmation of focal lesions is 84−96%, with a **specificity** of 86−100%. Differentiation between intra- and extrahepatic obstruction was successful in 77−97% of cases; the location of the obstruction was clarified in 79−98%, and the aetiology of the obstruction was established in up to 76% of cases.

1.8.1 Benign liver tumours

1. **Adenoma** is not characterized by any specific features in CT. Density varies between hypodense and slightly hyperdense. The contours are smooth. Following the administration of CM, brief and homogeneous accumulation mostly occurs in the adenoma with the appearance of an initially hypodense margin, which is enhanced in the late phase as a hyperdense border. However, contrast medium which is transportable in the bile cannot enter the adenoma, because it does not contain any biliary structures. An adenoma is frequently distinguished from FNH by evidence of necrotizing areas or sites of fresh bleeding; the latter are recognizable as hyperdense areas. (24, 26, 52)

2. **Focal nodular hyperplasia (FNH)** is distinctly circumscribed, usually round or oval in shape and isodense to slightly hypodense. As a rule, a predominantly hyperdense, central scar zone with stellate septa consisting of connective tissue is visible. Following application of CM (by i.v. infusion), equal concentrations are seen in the liver parenchyma and hepatic tumour, so that the latter may easily pass undetected. In contrast, following i.v. bolus injection of CM, a short, marked and homogeneous enhancement occurs, except in the central cicatricial area. • By means of hepatobiliary sequential scintigraphy, the diagnosis of FNH can be confirmed, particularly with regard to its differentiation from adenoma. (26, 34, 37, 42, 52) (s. p. 202)

3. **Cavernous haemangioma** is hypodense; in some cases, small hyperdense calcified foci are seen within the generally thrombotic centre. The contours of the haemangioma are usually smooth. Density is 35−55 HU. *Bolus injection of CM* is an important diagnostic tool. In the early phase (10−30 seconds), increased, predominantly irregular or garland-form enhancement is observed in the periphery, followed within a few minutes by a slow centripetal increase in density up to isodense values (so-called *"iris-diaphragm phenomenon"*). In the late phase (>10−15 minutes), even hyperdense values may be recorded with a parallel decrease in the density of the surrounding liver parenchyma. (s. fig. 8.5) Haemangiomas with a diameter of >1.0 cm can usually be diagnosed. Thrombotic or fibrotic processes within the haemangioma make differential diagnosis more difficult. (17, 32, 35, 40, 54) • *In our opinion, percutaneous fine-needle biopsy is not advisable!*

Fig. 8.5: Haemangioma (see arrow). Dynamic CT (contrast-enhanced); portal venous phase (s. figs. 6.18; 8.9; 36.7−36.9)

1.8.2 Vascular lesions

1. **Hepatic haematoma** mostly appears as a well-defined hypodense area; branching is seen in some cases. Intrahepatic haematomas are predominantly round-oval, whereas subcapsular haematomas are mainly crescent-shaped. Depending on their persistence, haematomas have different density values: initially, they are slightly hypodense (40−50 HU), but moderately hyperdense values can already be recorded after a few hours following the reabsorption of plasma. The values become more hypodense (10−20 HU) with increasing lysis and exceed 80 HU in the presence of calcification. Connective tissue generally shows values ranging from 50 to 60 HU.

2. **Liver injury:** Fresh bleeding can be reliably differentiated from a long-standing haemorrhage by CT, which is of importance in cases where surgical procedures are being considered. (33, 41)

3. **Liver infarction** generally leads to a sharply delineated, in most cases triangular, hypodense area, possibly extending up to the liver surface.

4. **Budd-Chiari syndrome** may be imaged in CT as hypodense zones; the findings are not reliable. (27) A definitive diagnosis can be obtained by angiography or MRI.

1.8.3 Hepatic cysts

1. **Dysontogenetic cysts** are solitary or multiple. They are clearly distinguishable from their surroundings, have smooth walls and are readily recognizable by their hypodense (water-equivalent) density values (0−20 HU). In the case of bleeding into the cyst, higher density values are recorded. (This also applies to infections of the cyst fluid or the occurrence of mucous contents.) Following i.v. application of CM, the cyst exhibits no increase in density (in contrast to metastases). A cystic liver is usually associated with cystic kidneys or cystic pancreas. (51) (s. figs. 6.13; 8.6; 36.11−36.14)

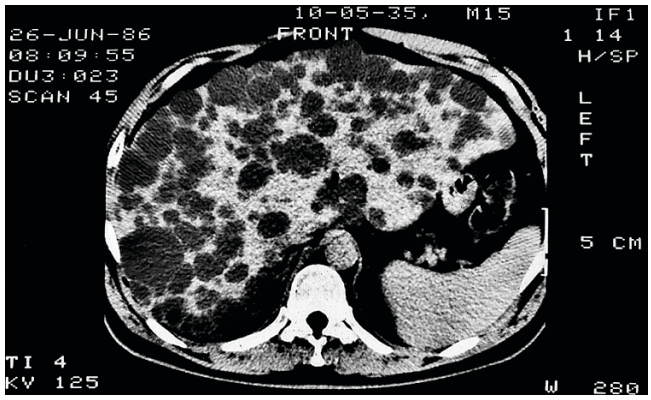

Fig. 8.6: Pronounced dysontogenetic cystic liver and cystic kidney

2. **Echinococcus cysticus** is generally visualized as a multilocular septate cyst with embedded secondary cysts. Both primary and secondary cysts are surrounded by inflammatory granular tissue. During the subsequent course of the disease, calcium deposition is seen in the cystic wall. The application of CM results in mural enhancement. The resulting demarcation of the cysts within the liver is relatively sharp. (8) (s. p. 510)

3. **Echinococcus alveolaris** presents a totally different picture: during the exocystic development of secondary cysts, the parasite gives the impression of growing in an infiltrative, destructive manner. CT scans reveal vaguely outlined, hypodense lesions of a cyst-like nature with nodular calcification (in most cases). Following the application of CM, an inhomogeneous increase in density is observed within the perifocal inflammation. Echinococcus alveolaris is, therefore, easily confused with malignant tumours. (s. p. 512)

4. **Caroli's disease** presents with multiple tubular structures, which correspond to focal cystic dilations of large interlobular bile ducts. The reduced density values of

these ectatic structures in CT are bile-equivalent. Intravenous application of a biliary CM provides the definitive diagnosis. Both portal fibrosis and portal hypertension are present. (16, 44) (s. pp 697, 785)

5. **Choledochal cysts** are congenital, segmental dilations of the larger intrahepatic bile ducts and/or the common bile duct. Diagnosis is obtained by i.v. administration of a biliary contrast medium. Choledochal cysts are frequently combined with tumours, so that additional corresponding signs of biliary obstruction may be verified by means of CT.

1.8.4 Inflammatory liver lesions

1. **Liver abscesses** are mostly (approx. 80%) localized in the right lobe of liver. A pyogenic abscess is visible as a hypodense lesion (0−30 HU) corresponding to the suppurative material with relatively sharp contours. It is surrounded by a hyperdense rim, caused by the well-vascularized granulation tissue. Should a perifocal oedema be present, it may produce an additional hypodense rim. Following the application of CM, an increase in the density of the hyperaemic and hyperdense abscess wall is observed, whereas the density of the abscess remains unchanged. Gas formations inside an abscess caused by anaerobes are easily recognizable on a CT scan. The success rate for detection is 95%. (s. figs. 6.14; 9.2; 25.1; 27.1) *(see chapter 27)*

2. **Macronodular tuberculosis** as screened by CT may be very problematic with respect to its differentiation from benign or even malignant liver tumours. (19, 21)

1.9 Malignant liver tumours

Most malignant liver tumours are hypodense; the difference in value to normal liver parenchyma is usually 15−25 HU. Evidence of hepatic malignancy is obtained by CT, especially by CTAP, in approx. 85% of cases with tumours of >0.5 to 1.0 cm in diameter. (50, 53)

1. **Hepatocellular carcinomas** are extremely variable on CT scans because of their different forms of growth. Morphologically, they appear as (*1.*) isolated masses, (*2.*) multinodular infiltration, or (*3.*) diffuse parenchymatous infiltration. In addition to the mainly hypodense areas, hyperdense regions are also distinctly visible. The often somewhat irregular and slightly blurred, but nevertheless clearly hypodense border shows marked enhancement under CM. Space-occupying lesions, hitherto unrecognizable, may become discernible at this point. Evidence of hypodense areas in liver cirrhosis always strongly suggests primary liver carcinoma. Segmental or lobar decreases in density as a result of frequently occurring infiltrations of the portal vein indirectly suggest the presence of a tumour. Lymph node metastases can also be detected. It is much easier to recognize involvement of the vascular system with the help of CTAP or spiral CT. Depending on the size and location of the hepatocellular carcinoma, contour bulging is also observed. The sensitivity is approx. 75%. CT is an indispensable feature in planning surgery. (5, 28, 30, 31)

2. **Liver metastases** are frequently multiple. They vary in size and are usually hypodense. In contrast to liver parenchyma, they display relatively sharp contours, with a difference in density of at least 10−15 HU. In fatty liver, metastases may even appear hyperdense. Liver metastases are mainly supplied by arterial blood. Therefore i.v. (or even intra-arterial) bolus injection of CM produces the best diagnosis: the metastasis shows increased CM enrichment during the short hypervascular phase; additionally, a peripheral margin forms as a result of the increased concentration of CM. Metastases of 5−10 mm can be detected. Data in the literature confirm a *sensitivity* of 65−91% (in breast cancer up to 100%) and a *specificity* of 81−92%, giving a detection rate of 80−85%. Proof of metastases clearly depends on the histology of the primary tumour; the best diagnostic results are obtained in breast and colon carcinomas. (22, 40, 50, 53, 57)

3. **Malignant lymphomas** may appear in the liver as focal, hypodense lesions. By contrast, diffuse impairment of the periportal region is only demonstrable with CT using special CM. Additionally, extrahepatic lymphomas can be detected at the same time.

1.10 Bile duct obstruction

Obstruction of a large bile duct leads to dilated intrahepatic bile ducts, which appear on CT scans as ramified linear or rounded structures with bile-equivalent density. Their luminal diameter increases progressively in the direction of the hilus. (47) Segmental dilation of the bile ducts may be indicative of a tumour. A dilation of the bile duct of >9 mm points to a peripheral obstruction, mostly near the papilla of Vater.

1.11 Surgical therapy

Pre- and post-therapy CT examinations must be carried out in resections and transplants as well as arterial ligatures, embolization therapy with or without chemotherapy, and also regional chemotherapy. Haematomas, seromas and abscesses can occur around the edge of the resection; compensatory hypertrophia from the residual parenchyma can be identified if no complications occur. After a transplant, hypodensities may point to complications (e. g. necrosis, infarctions, rejection foci). Portal veins enhanced by accompanying hypodense lines are a sign of rejection. Postoperative fluid in the abdomen can also be easily detected using ultrasound and computer tomography. Thromboses in the hepatic artery are discernible with the aid of dynamic CT.

The strategy generally applied in diagnostic clarification in a case of suspected **"liver tumour"** is shown later in a **flow diagram.** (s. p. 204) (s. fig. 9.4)

2 Magnetic resonance imaging

► Magnetic resonance imaging (MRI) − also known as magnetic resonance tomography (MRT)− was introduced into medical diagnostics by P.C. Lauterbur in 1973.

2.1 Principle

The production of a strong magnetic field induces alignment of the protons along this magnetic field. The homogeneous alignment is perturbed by appropriate high-frequency signals. The protons are diverted and set in a spinning motion. As a result of their efforts to return to the original position, energy is released, which is registered as a signal, calculated by computer analysis and converted to images. The resulting MR signal is dependent on hydrogen nuclei in the object and on the tissue-based time constants T_1 and T_2, i.e. the signals can deviate from the norm (= **isointensive**) by being either **hypointensive** or **hyperintensive**. In this way, (*1.*) tissues with different proton density values can be distinguished, (*2.*) concentrations of body-own elements (C, F, N, P) can be determined, and (*3.*) chemical compositions of certain tissue areas are clarified by means of supraconductive apparatus with magnetic fields of 0.5−2.0 tesla (T).

Four parameters are thus imaged in MRI by means of mathematical calculations: (*1.*) *proton density*, (*2.*) *relaxation time* T_1 (= binding force between the nuclear spin grate and the surrounding molecular grate), (*3.*) *relaxation time* T_2 (= binding effect between the various nuclear spins), and (*4.*) *flow velocity.*

Two types of appliance are used: (*1.*) resistance (or iron) magnets and (*2.*) supraconductive magnets.

Paramagnetic substances such as manganese or gadolinium compounds (Gd-DTPA, Gd-EOB-DTPA, Gd-BOPTA, Gd-DOTA of Mn-DPOP) are used as i.v. contrast media. They are absorbed by the hepatocytes, so that healthy liver tissue appears lighter on T_1 images ("whitener" effect). These substances are excreted via the biliary and renal system. • **Superparamagnetic particles of iron oxides** (SPIO) is a new contrast medium for exact localization of focal liver lesions and for differentiation of normal and pathological regions. The 3−5 nm iron oxide nuclei grow to a size of 45−60 nm due to the polysaccharide sheath. They are principally absorbed by the RES (but also collect temporarily in the extravascular space). These iron oxide nuclei are broken down into lysosomes and taken into normal iron storage; the respective iron uptake corresponds to the average nutritional intake of two to three days. Healthy liver tissue appears as dark areas in T_2 images ("darkener" effect). This shows that CM is also stored in the fatty liver and FNH. Foci of up to 2−3 mm can be detected. Hepatic metastases appear extremely "light" compared to the "black" parenchyma. (62, 84, 89, 97, 103, 122)

2.2 Advantages

These techniques can be used to achieve a very *sharp contrast between various tissues.* This permits better differentiation and characterization of normal or pathological tissues, compared with ultrasonography and CT. • A great advantage of MRI is the possibility of imaging not only transverse *cross-sections* (as is the case with CT), but also *longitudinal sections* of various planes (e.g. sagittal and coronary) in the hepatic area − without changing the patient's position. Topographic analysis and the interpretation of findings are hence less complicated than with CT. The thickness of the section planes is usually 10 mm. • MRI is also capable of differentiating static from flowing conditions and calculating the *flow rate* in various vascular areas. • Furthermore, the concentration of certain *elements* and the *proton density* can be measured. MRI is thus a valuable diagnostic tool in certain situations, serving to supplement CT and at the same time replacing intra-arterial angiography or scintigraphy. • A further major advance is the development of **MR angiography** − which may well prove to be a (better) alternative to invasive catheter angiography. (99)

2.3 Disadvantages

The use of first-generation MRI was associated with certain problems, e.g. **artefactual images** caused by respiratory movement, cardiac action, vascular pulsation and intestinal peristalsis. The introduction of turbo-spin-echo-pulse sequences, however, led to a drastic shortening of recording periods, so that artefacts due to breathing and peristalsis are now rare. It is important that the patient breathes normally and is in a resting position. In addition to the reduction in recording periods with modern apparatus, the time needed for reconstruction has been shortened thanks to new computer imaging techniques (polytomography, 3D-layer batch). • Thought should be given in this respect to the **physical stress** experienced by the patient through a static magnetic field, temporally varying magnetic fields and high-frequency fields in the megahertz range. No clinically significant damage has been reported if attention is paid to the contraindications. • In individual cases, the time spent in the magnetic tunnel may, however, cause **mental distress.** Sometimes this claustrophobia requires sedative premedication. In order to suppress **intestinal peristalsis,** administration of spasmolytics or glucagon (0.5 to 1.0 mg i.v.) is recommended. • The operators should be aware of potential **contrast-medium incidents.** In practice, however, such adverse reactions are rarely seen.

Contraindications are internal *ferromagnetic objects* in the body, e.g. implants, clips, splinters and especially cardiac pacemakers. Through their electromagnetic effects, they may cause biomolecular disturbances, and even cellular damage. Based on the current level of knowledge and the developmental stage of the technical equipment and contrast media, it is advisable that *pregnant women* and *nursing mothers* as well as *epilepsy patients* be generally excluded from MRI examinations (however, such contraindications become relative in the face of a strong indication).

2.4 Normal liver

On MRI scans, a normal liver generally produces a picture similar to that obtained by CT. The parenchyma appears as a homogeneous area with relatively high signal intensity (T_1). The portal and liver veins are easily differentiated as signal-free or low-signal structures. With prolonged echo-time, the signal intensity of the liver veins also increases. (s. fig. 8.7)

Fig. 8.7: Normal MRI: **a**) T_1-weighted scan; **b**) T_2-weighted scan. • Branches of the portal vein (→), aorta (---▶), spleen (S), inferior vena cava (⇒) with stellate ramifications of the hepatic veins

2.5 Diffuse liver diseases

Acute hepatitis: In the early stages of the disease, the T_2-scan shows an increase in signal intensity, whereas a prolongation of T_1 tends to be observed before the occurrence of liver cell necrosis.

Fatty liver: Fatty infiltration into liver cells is not detected by MRI, even though fatty tissue shows high signal intensity on spin-echo imaging. The water associated with the (hyperdense) fatty liver may lead to a signal reduction during the T_1-time, whereby the plus and minus variations in signal intensity result in an indifference, which corresponds to normal liver tissue; T_1 and T_2 thus remain unchanged. Only markedly T_1-weighted scans exhibit increased signal intensity. MRI is an important method in searching for (hypodense) metastases in a (hyperdense) fatty liver. (39, 89) (s. p. 138, 180)

Cirrhosis: Like CT, MRI also portrays cirrhosis-related changes in liver size and shape, irregular superficial contours, dilated portal vessels and collaterals (generally also reversal of portal flow) as well as splenomegaly. As a result of the enhanced blood engorgement, the spleen shows a clear increase in signal intensity. Regeneration nodes are distinguishable because the T_1 and T_2 signal is weaker here than in cirrhotic tissue. So-called siderotic nodes are found in 25% of cases ($T_2 \downarrow$). Malignant foci do not contain any iron. This results in "nodes within nodes", where malignant growth occurs in a regeneration node. (86, 92, 93, 96, 107)

Haemochromatosis: Due to the accumulation of iron in the liver cells, the relaxation time T_2 is much shorter and the signal intensity weaker. This can also be determined quantitatively. Depending on the iron content, the liver appears dark grey to black. (s. fig. 8.8) The detection rate is 100% at an iron concentration of 1 mg/g liver tissue. An iron-free node may suggest HCC. • *Haemosiderosis* with iron deposition in the RES is characterized by similar, yet less marked findings. A fall in signal intensity is discernible when the iron content/g in the liver tissue has almost quadrupled. (58, 64, 78, 91, 94, 113)

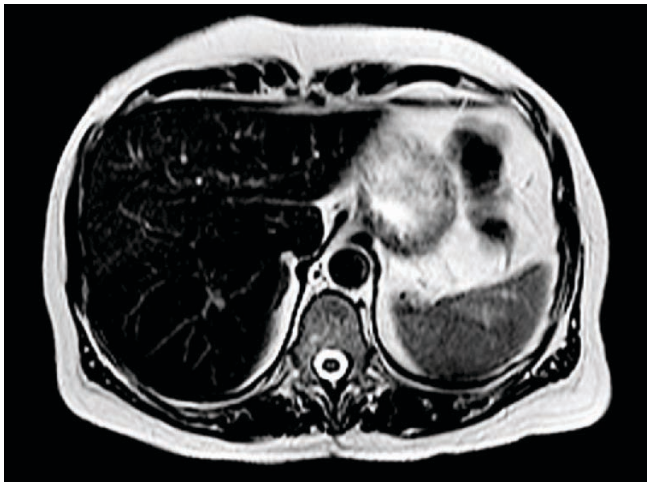

Fig. 8.8: Haemochromatosis: characteristically weakened signal (or even signal elimination) in a T_2-weighted scan due to disturbances in the magnetic field caused by iron deposition in the liver

Primary biliary cirrhosis: In correspondence with the extent of copper deposition in the liver, the relaxation times T_1 and T_2 are shortened, with a distinct decrease in signal intensity. (121)

Others: Further study results are available relating to amyloidosis (29, 111), primary sclerosing cholangitis (73), peliosis hepatis (105), Budd-Chiari syndrome (29, 60, 108), schistosomiasis (29, 79), biliary tract diseases (75, 82, 120), echinococcosis (69, 71) and adenoma. (67, 74)

2.6 Focal liver lesions

Focal liver lesions of >2 mm in diameter are detectable in MRI. In addition, the specificity of MRI is higher than can be achieved by means of CT examination. (2, 29, 61, 62, 89, 97, 106, 119)

Cavernous haemangioma: The visualized findings consist of a roundish, homogeneous high-signal (T_2-weighted *"light bulb"*) area and a well defined hypointense to iso-

intense (T_1-weighted) area. (s. fig. 8.9) Usually, no internal structures are visible. The imaging effect is best accomplished following i.v. administration of Gd-DTPA on the T_1-weighted scan with centripetal contrast-medium enhancement. Because of the paramagnetic component of methaemoglobin, the signal intensity may be more pronounced, although it is usually reduced in a T_1-weighted scan. (63, 76, 83, 87, 101, 110, 114, 116)

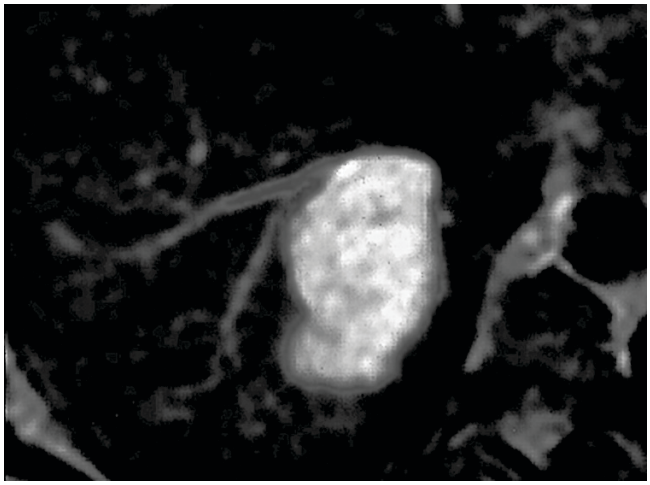

Fig. 8.9: Cavernous haemangioma: a large (2.5 × 4.2 cm) hyperintense (white) lobular focus with an afferent vessel (T_2-weighted scan; transverse) (s. figs. 6.15; 8.5: 36.6)

Focal nodular hyperplasia: On MRI scans (as with CT), FNH shows the characteristic central venous star. Otherwise, the signal intensity of FNH is homogeneously isointense (T_1) or slightly hyperintense (T_2). Immediately following the i.v. administration of CM (Gd-DTPA), a distinct but rapidly fading enhancement is observed. (65, 95, 100, 102, 110, 118)

Malignant tumours: Due to their prolonged relaxation times, malignant tumours are sharply demarcated from the liver parenchyma. On T_1-weighted scans they are low-signal, on T_2-weighted scans they are high-signal areas. Differentiation of tumour tissue from central necrosis is possible. Intrahepatic, tumour-induced vascular displacements as well as capsular structures and perifocal oedema can be demonstrated. This is characterized by an intact ring of enhancement on hepatic arterial dominant-phase images. There is sometimes a peripheral or heterogeneous washout of contrast agent in the hepatic venous phase or a washout leading to hypointensity, even in hypervascular metastasis. It is not (yet) possible to define the tumour type. Moreover, differentiating malignant tumours from adenomas (67, 74) and haemangiomas (76, 87, 101) or from focal fatty infiltration (39) is problematic. The success rate for differentiating patients devoid of liver tumours from those with metastatic liver is 87% (CT: 84%) with a specificity of 98% (CT: 91%). (70, 97) • Proof of metastases (23, 29, 39, 66, 70, 72, 76, 87, 101, 102, 117, 119) (s. fig. 8.10) or hepatocellular carcinomas (29, 66, 68, 80, 81, 85, 90, 96, 98, 112) is obtained in 85−95% of cases. Study results in patients with cholangiocarcinoma (77), mesenchymal tumours (104, 109) and plasmocytoma are also available. Small-nodular carcinosis in the omentum or peritoneum (without concomitant ascites) and subcapsular hepatic metastases (< 5 mm) remain undetected with US, CT or MRI − they can only be found using laparoscopy.

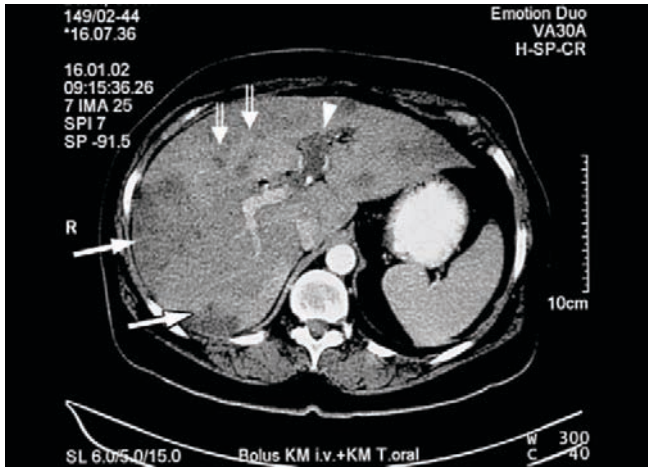

Fig. 8.10: Multiple metastases of a pancreatic carcinoma (↑); numerous focus-like signs of aerobilia (↟); thrombosis of the left portal vein (▲)

Hepatic cysts: Cysts are visualized on the T_1-weighted scan as low-signal (= black) and on the T_2-weighted scan as homogeneously high-signal (= bright), closely circumscribed, focal lesions. An increase in signal intensity on the T_1-weighted scan suggests bleeding into the cysts.

Hepatic abscesses: An abscess is displayed as low-signal in the T_1 image and signal-intensive in the T_2 image. The perifocal oedema cannot be separated from the lesion. Gadolinium CM can be used to visualize a thick abscess wall in the T_1 image. Gas appears hypodense and cannot be differentiated from prior bleeding. • Treatment of such abscesses is easily monitored.

Portal veins: There are reports on MRI visualization of large intrahepatic portovenous shunts (59), collaterals in the portal vein (92, 115) and VOD staging. (88)

The strategy generally applied in diagnostic clarification in a case of clinical suspicion of **"liver tumour"** is shown later in a **flow diagram.** (s. p. 204) (s. fig. 9.4)

3 Angiography

For clarifying vascular liver diseases and alterations of vessels associated with liver diseases (especially tumours), angiographic procedures are available, should CEDS, CT and MRI yield no definitive diagnosis. With the help of contrast media, they make possible the imaging of the afferent arterial or portal vessels and the efferent veins in the area of the liver. (s. tab. 8.3)

Arteriography
1. Coeliac artery (coeliac trunc Halleri) (s. fig. 8.11)
2. Selective arteriography
   - common hepatic artery
   - superior mesenteric artery
   - splenic artery
   - right/left hepatic artery

Portography
1. Direct splenoportography
   – percutaneous (s. fig. 8.12)
   – laparoscopic
2. Indirect portography
   – splenoportography via the splenic artery
   – portography via the superior mesenteric artery (s. fig. 8.11)
3. Omphaloportography (s. fig. 8.13)
4. Transhepatic portography

Phlebography
1. Cavography
2. Phlebography of the hepatic veins
3. Transhepatic phlebography

Tab. 8.3: Angiographic liver examination methods which are possible in principle, but which are now partially obsolete

3.1 Arteriography

► Selective arteriography uses a transfemoral catheter technique (S. I. Seldinger, 1953; P. Ödman, 1959). (s. fig. 8.11) • The catheter may also be introduced into the axillary artery. Superselective CM visualization of hepatic arteries via the proper hepatic artery shows blood vessels down to the sixth division; the smallest depictable diameter is approx. 0.5 mm. Imaging of the arteries is effected by nonionic iodine-containing contrast medium at a reduced flow rate (20–30 ml, 6–8 ml per second). Using this infusion technique, 8 to 12 angiograms can be produced within a period of approx. 12 seconds. In this way, both the early arterial phase and the parenchymal phase as well as the venous phase can be recorded. Visualization of the CM-filled blood vessels is effected by (*1.*) *conventional film angiography* which has been replaced by digital subtraction angiography, (*2.*) *digital subtraction angiography* (DSA) using an image-intensifying TV link instead of the X-ray film, (*3.*) *CT arterioportography,* or (*4.*) *MRI angiography* and meanwhile *whole body MR arteriography* using gadolinium. (133)

3.1.1 Indications

Focal liver lesions of >1.0–1.5 cm in diameter are usually detectable. Even hypervascular foci with a diameter of >0.5 cm are visible when using the infusion technique. In 75–90% of cases, a normal arterial blood supply is guaranteed via the proper hepatic artery. Alterations relating to the hepatic arteries can be angiographically confirmed in virtually 100% of cases. Vascular anomalies (10–20%) are of no clinical significance. Knowledge of their existence may, however, be important in surgical procedures. Variations in the location and shape of the liver and changes in the region of the caudate lobe and quadrate lobe are also recognizable. Despite the initial use of noninvasive imaging methods, and possibly laparoscopy, hepatic arteriography is still indicated in some situations, especially for the purpose of *angiotherapy.* (123, 124, 128, 135, 136, 141, 145, 147, 148, 151, 157) (s. tab. 8.4)

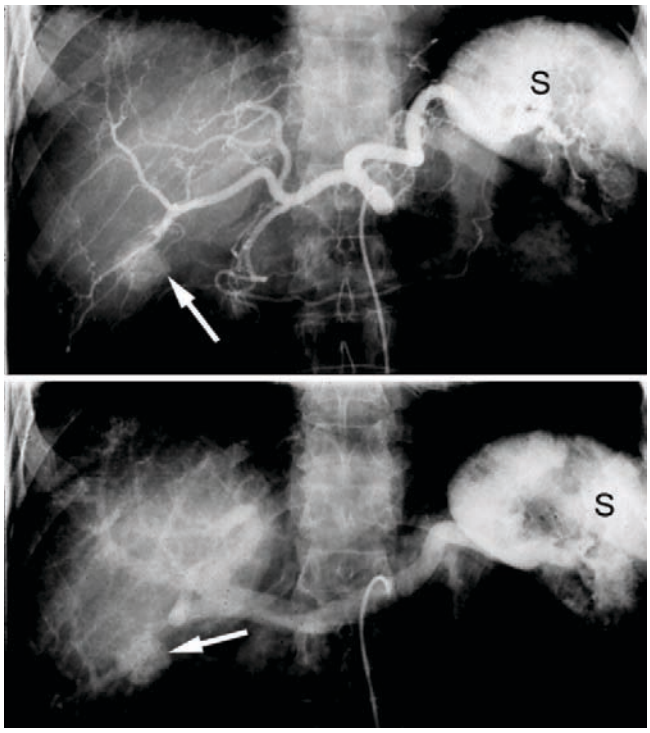

Fig. 8.11: Arterioportography: coeliacography with good visualization of the branches of the coeliac trunk including the fine ramifications. Small hypervascularized haemangioma (↑); S = spleen. (The pancreatic vessels are also visible.) • Normal depiction of the portal vessels in the venous phase

1. Vascular anomalies, stenoses or aneurysms
2. Preoperative study of vascular blood supply
3. Haemobilia
4. Arteriovenous fistula
5. Occlusive (including posttraumatic) embolization
6. Angiotherapy within the framework of a transjugular intrahepatic portosystemic stent shunt (TIPS)
7. Treatment of liver tumours
   – chemoinfusion, chemoperfusion, chemoembolization

Tab. 8.4: Possible indications for hepatic arteriography if modern contrast-medium-based CEDS, CT and MRI fail to provide reliable information, or if angiotherapy is indicated

3.1.2 Contraindications

Hepatic arteriography is contraindicated in cases of severe *coagulation disorders.* Cut-off values are deemed to be: Quick's value of >60%, thrombocytes of >100,000, and bleeding time of <3 minutes. These figures only serve as a guide; a more careful assessment must be made in each individual case. • In the presence of *renal failure*, the use of contrast media, and thus arteriography, is contraindicated.

3.1.3 Complications

With strict heparinization, the incidence of serious complications is below 1%. A lethality rate of 0.06% has been reported. Arterial puncture is associated with certain risks relating to the introduction of a guide wire or

catheter (thrombosis, formation of haematomas, arteriovenous fistula) and to the catheter itself (damage to the vascular wall, thrombosis, vascular perforation). Intolerance reactions to the contrast medium may also occur (in 3–5% of cases). With DSA, however, the complication rate decreases.

3.1.4 Focal lesions

In the diagnosis of focal liver lesions, angiography is no longer of any real practical value. The angiogram of focal liver lesions is usually nonspecific. • *With regard to its indications, hepatic arteriography has lost importance as a diagnostic tool, but has become more valuable as a therapeutic approach.* • Hypervascular foci and foci situated in the peripheral liver sections are identified more reliably than those in the central areas. The intermediary region between the right and left lobe of liver shows less vascularization; additional vascular supply variants are seen here more often. In hypervascular tumours, the success rate for detection is >90%. This is further improved by the use of angio-CT.

Primary malignant liver tumours with a predominantly hypervascular blood supply mainly comprise carcinomas and sarcomas. Depending on the vascularization of the tumour, the parenchymal phase shows areas that are lower in CM density and others with increased CM density (*"pooling"*). Where there is insufficient blood flow, this pooling often results in patchy images. • The *criteria of malignancy* are neovascularization, irregular outline, "vascular break-offs", "blood lakes" as a result of dilated vessels, early discharge of contrast material via arteriovenous anastomoses in pathological veins, vascular occlusions, increase in the calibre of nutritive hepatic arteries, reduced intratumoural circulation, corkscrew-shaped arteries of different calibres, and vascular displacements (stretching, spreading or arciform displacement of arteries). Cholangiocellular carcinomas and the hepatocellular carcinomas related to liver cirrhosis are mainly hypovascular. For this reason, they are hardly recognizable. (130, 139, 144, 149–151)

Secondary malignant liver tumours, such as metastases of adenocarcinomas, are also hypovascular and therefore usually not identifiable by arteriography. In contrast, the metastases of malignant goitre, hypernephroid carcinoma, insulinoma and chorionepithelioma are hypervascular and therefore readily visible.

Benign focal lesions usually lead to a smoothly curved displacement of arteries (and veins). In the parenchymal phase, they show more or less sharply delineated filling defects. (132, 145, 156)

In 80–90% of cases, *focal nodular hyperplasia* shows a typical, radial (spoke-like) arrangement of coiled vessels in the area of the tumour, which originate from a circular artery. Occasionally, fine a.v. shunts are present. The smooth-edged lesion is hypervascular. The parenchymal phase, with its homogeneous concentration of contrast medium, allows the lesion to be clearly demarcated from healthy liver tissue. (156) • *Hepatic adenoma* is generally hypervascular. Displaced vessels are frequently visible. A nutritive vessel extends into the tumour from the periphery. Neovascularization and irregularities of the vessels may be shown, which complicates differential diagnosis with regard to malignancy. In the parenchymatous phase, the tumour exhibits marked enhancement. (156) • The *cavernous haemangioma* shows late filling of the hollow spaces; the contrast medium initially accumulates in the form of lacunes at the margin of the tumour. Patchy, blurred outflows of contrast material subsequently appear in the whole tumour area. The contrast medium persists for an extremely long period of time into the parenchymatous phase. No arteriovenous fistulas are detected. (129) • Intrahepatic *haematomas* lead to separation of the major vessels with vascular break-offs and extravasations. Arteriovenous shunts may occur. There is no visualization of the parenchyma. • *Haemobilia* is characterized by an arteriobiliary flow of CM with imaging of the intra- and extrahepatic bile ducts. (142) • *Echinococcus alveolaris* with its invasive and multilocular growth produces an image similar to that seen in malignant liver tumours. At the periphery, irregular, often twisted and stenotic or occluded arteries and small CM extravasations are visible. In the parenchyma, contrast medium-free areas as well as occasional CM enhancement can be detected.

3.1.5 Diffuse liver diseases

Arteriography is not a suitable method for diagnosing **liver cirrhosis.** It may only be used in special situations (e. g. planned surgical procedures). In liver cirrhosis, the arteries appear dilated in some cases or take the form of narrow vessels; mostly, the arterial presentation is sparse. At the periphery, the arteries often follow a spiral course. The parenchymal phase exhibits an inhomogeneous, patchy image; regions with connective tissue appear hypovascular. Regeneration nodes can resemble benign liver tumours in arteriograms. In advanced stages of cirrhosis, the hepatic artery may dilate as a result of increased arterial flow, with a subsequent reversal of the flow in the gastroduodenal artery. The latter is therefore no longer visible in coeliacography. In patients with cirrhosis showing dilation of the hepatic artery and a reversed blood flow in the gastroduodenal artery, the blood circulation and functions of the liver are better than in patients without this "steal effect". *Such a finding may be an important criterion when considering a portacaval shunt operation.* (123, 127, 141, 143)

3.1.6 Therapeutic infusion

In traumatic bleeding in the area of the liver, haemostasis may be performed within the framework of diagnostic arteriography by means of embolization. Arterial access likewise facilitates embolization and cytostatic treatment of liver tumours (following angiographic insertion of the catheter). (s. tab. 8.4)

3.2 Portography

► In animal experiments, a contrast medium was first injected percutaneously into the spleen by S. Abeatici et al. in 1951 in order to visualize the portal circulation by means of X-ray. This method was later introduced into clinical practice as direct splenoportography by J.L. Leger (1951) and R. Boulvin et al. (1951).

Portography is defined as the radiological visualization of the portal vein and its various afferent branches as well as their distribution in the liver. (s. tab. 8.3) It facilitates not only the direct measurement of portal pressure, but also the exact localization of portal flow obstruction and thus the differentiation between prehepatic, intrahepatic or posthepatic block. The prehepatic block can be located at the edge of the splenic and/or portal vein. Blood flow is predominantly in a hepatopetal direction. Central blocks are frequently the result of an infection in the umbilical vein during early childhood. (s. p. 190) This usually leads to cavernous transformation of the veins in the hepatoduodenal ligament and the formation of periportal veins. An intrahepatic block results in hepatofugal blood flow. Portal high pressure can be recognized in the early stages by a widening of the left gastric vein (> 5−6 mm). For surgical planning in portal hypertension, knowledge of portal vascular morphology and haemodynamics is a major prerequisite. • Shunt function, blood flow to the liver and collateral circulation are accurately displayed with the aid of indirect mesenteric and splenic portography. In more difficult cases, the shunt can be monitored using a direct probe via the inferior vena cava. (128, 137)

Impressive images of portal arteries and hepatic veins can be produced by MR angiography. (131, 152) Nowadays, CM-supported MRA is the method of choice in monitoring the portal artery system (primarily before and after TIPS insertion). (152)

3.2.1 Indications

Ultrasound and, more particularly, colour-encoded Doppler sonography are the methods of choice for the diagnostic study of the portal venous system. • Equivocal findings are an indication for contrast-medium CT or MRI, both of which provide superior angiographic images following i.v. injection of an appropriate CM − this is equally possible on an outpatient basis. • Portographic examination techniques should only be used in special instances which are not sufficiently clarified by these imaging procedures. The various techniques may have different indications in individual cases. The appropriate method should be carefully selected; this depends to a large extent on patient-related considerations. (s. tabs. 8.3, 8.5)

1. Differentiation of various forms of portal hypertension, with measurement of blood pressure if necessary
2. Checking on the possibility of anastomosis in portal vessels
3. Detection of spontaneous splenorenal shunts
4. Proof of collateral flow in bleeding oesophageal varices
5. Follow-up after shunt operation
6. Suspected Budd-Chiari syndrome
7. Identification of the morphological course of hepatitis (with variations between the single segments)

Tab. 8.5: Potential indications for portography if modern contrast-medium CEDS, CT and MRI fail to provide reliable findings

3.2.2 Direct splenoportography

1. **Laparoscopic splenoportography** has three **advantages** over the percutaneous technique (153): (*1.*) splenic puncture is performed under visual control, (*2.*) the procedure can be repeated several times during the same examination, and (*3.*) complications are rare. • The **examination** itself is not subject to time pressure, thus permitting measurement of the "standing" blood column with imaging up to ten minutes and longer following the injection of contrast medium. The needle is inserted from the medial splenic margin 4−5 cm deep into the caudal or medial segment, axially and in the segmental central line. The correct positioning of the needle in the spleen can be checked by the **decholine test,** which also provides information on the portal circulation. With open arterial crus and simultaneously closed venous crus or with both vascular crura open (filling and flow phases), pseudoarterial afterbleeding lasting for ten minutes or longer may occur, which spontaneously ceases when there is a change in phase from filling to emptying. Coagulation measures are advisable in prolonged secondary haemorrhage.

2. **Laparoscopic transhepatic retrograde splenoportography** allows early diagnosis of portal hypertension by segmental portography of the liver. The puncture cannula is correctly positioned in a portal vessel when the injected contrast medium is distributed like the crown of a tree and the measured portal pressure (normal 8−15 mmHg) exceeds the pressure of the hepatic vein (normal: 4−8 mmHg). • **Direct splenography using laparoscopy also allows identification of different morphological alterations in various segments!** (153, 154) *Particular consideration must be given to this factor when assessing a liver biopsy specimen.* • With laparoscopic angiography, both *segmental portography* and *segmental arteriography* have proved effective. (155)

3. **Percutaneous splenoportography** has lost its importance. Should a direct procedure be indicated, laparoscopic splenoportography is a possible alternative. Recently, a **new technique** has been described. (134) • The percutaneous splenic puncture is performed using a thin needle under screen control, with the needle directed at the splenic hilus. The pressure of the splenic pulp can be measured directly in order to estimate the portal vein pressure. Contrast medium is injected manually or by a special device. From this depot in the red pulp, the splenic vein, the portal vein and the intrahepatic branches of the portal vein are contrasted within a few seconds. (s. fig. 8.12) • *Complications* resulting from percutaneous splenoportography include afterbleeding from the spleen, bilateral rupture of the spleen, arterial aneurysms and a.v. shunts − these complications are serious in nature, but rare. • *Contraindications* for the procedure should be carefully observed. (s. tab. 8.6)

1. Clotting disorders
2. Ascites
3. Adhesions, especially perisplenic adhesions
4. Inoperability with respect to a shunt procedure
5. Splenic diseases (cysts, tumours, leukaemia, *etc.*)

Tab. 8.6: Contraindications for direct (particularly percutaneous) splenoportography

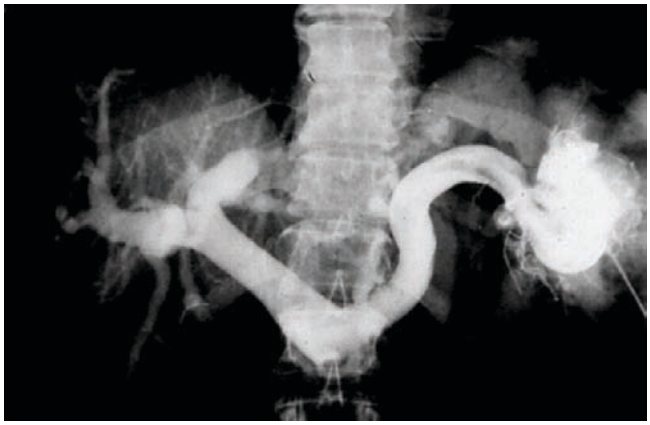

Fig. 8.12: Use of direct percutaneous splenoportography in portal hypertension

3.2.3 Indirect splenoportography

Except where there are individual unresolved diagnostic issues, direct portography has been replaced by arteriography. Using selective arteriography, the same examination yields (in 80−90% of cases) an indirect splenoportogram through the splenic artery and an indirect portogram via the superior mesenteric artery. In addition, the hepatofugal collaterals are shown, so that it is possible to assess the hepatic block and the direction of the blood flow. Portal pressure cannot be measured by means of this technique. • Following injection of a contrast medium into the coeliac trunk, the CM flows through the splenic artery into the spleen and returns through the splenic vein. Thus, in addition to the arterial system, the portal vein with its extra- and intrahepatic branches is also visible. (126) (s. fig. 8.11) • The *contraindications* and *complications* valid for any transfemoral catheterizations apply equally to indirect splenoportography. The low frequency of complications together with a good diagnostic yield make indirect splenoportography useful in clarifying specific issues. • In the case of severe **splenomegaly,** the attempt to visualize the splenic vein via the splenic artery usually fails, even with high doses of contrast medium of 60−80 ml − the CM simply "sinks into" the large spleen. In these cases, direct splenoportography is the method of choice.

3.2.4 Omphaloportography

Umbilical portography was first described by D. G. Duviner in 1954 and introduced into clinical use by O. Gonzales Garbalhaes in 1959. The umbilical vein consists of a right branch (which is totally obliterated postpartum) and a left branch (the cranial portion of which is closed, whereas the section in the vicinity of the liver is only sealed by endothelium); the latter is frequently preserved as a residual channel. The omphaloportographic **technique** is based on the surgical opening (at a point 5−7 cm above the umbilicus) and bouginage of the umbilical vein, with the subsequent insertion of a catheter. The probe is successful in 90% of cases. The (specially shaped) catheter can be inserted as far as the splenic or mesenteric vein. By injecting a contrast medium, the portal venous system is successfully imaged. (s. fig. 8.13) Visualization of single portal branches may be attempted using special catheters. Portal vein pressure can be measured directly. **Indications** are rare. It is, however, possible to determine the pressure in the portal vein directly (e. g. prior to shunt operations). (138) In the case of suspected apudomas, blood samples can be taken from the splenic vein for hormone analysis. It is also possible to use high-dosage chemotherapy (e. g. in colorectal liver metastases). In a laparotomy, omphaloportography may be useful for clarifying certain issues in isolated cases. (s. tab. 8.7) • Potential **complications** include perforation, thrombosis and infection. The complication rate is 10−15%. (138, 146)

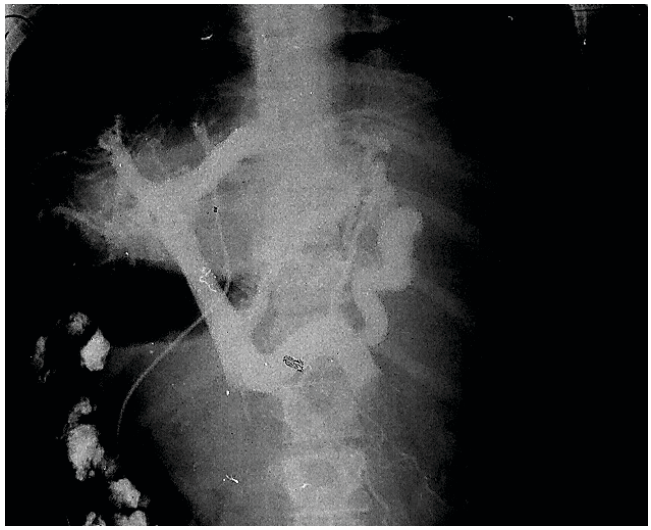

Fig. 8.13: Use of omphaloportography in portal hypertension

1. Preoperative diagnosis prior to liver resection or shunt operation
2. Status after thrombosis of the splenic vein or after splenectomy
3. Suspected "pseudo-obstruction" of the portal vein
4. Use of an extracorporeal makeshift vessel
5. Diagnosis directly from portal blood (e.g. measurement of portal pressure, apudoma)
6. Therapeutic instillation into portal blood (e.g. targeted high-dose chemotherapy in colorectal liver metastases)

Tab. 8.7: Indications for omphaloportography which are possible in principle, but now largely obsolete

3.2.5 Percutaneous transhepatic portography

This method was developed as an alternative to laparoscopic transhepatic portography. Some 40 ml of CM are usually injected at a rate of 10 ml/sec. It is a difficult technique, takes more time and involves greater risks. This method allows the portal pressure to be measured. After positioning the catheter with the aid of a guide wire, any branch of the portal vein can be visualized in a superselective manner following application of CM. This method can also be used to take blood samples from various veins for the purpose of hormone analysis. If oesophageal variceal bleeding occurs, targeted obliteration of the coronary vein is possible. Existing collaterals, including splenorenal connections, can be visualized. The frequency of severe complications (e. g. bile peritonitis, bleeding) is 2−3%.

3.3 Phlebography

The venous system of the liver can also be shown by X-ray. (s. tab. 8.3) Such radiological methods have their specific diagnostic yields and thus their own indications. (125, 131, 140, 158)

1. **Cavography** may be useful in patients with suspected Budd-Chiari syndrome or anomalies of the hepatic veins as well as prior to liver transplantation and in clarifying the aetiology of a posthepatic block. Cavography can be performed both through the femoral vein and inferior vena cava and through the arm or jugular vein via the right atrium and superior vena cava.

2. **MDCT venography** with a 16-row scanner provides detailed anatomical information in the evaluation of the three main branches of the hepatic vein. This is very important both for the donor and the recipient before LDLT, but also before and after LT. MDCT venography is a valuable diagnostic tool in other entities such as BCS, TIPS, intrahepatic venous shunt or hepatic venous involvement in the case of different tumours. (158)

3. **Transvenous hepatophlebography** is based on experimental studies in dogs and on initial clinical experience (A.M. Rappaport, 1951). This radiological method for imaging the hepatic veins was introduced into clinical practice by G. Tori in 1953. Selective hepatography introduces a catheter through the femoral vein (also via the median cubital vein or jugular vein) into a hepatic vein.

4. **Percutaneous transhepatic hepatophlebography** involves a typical puncture of the liver with a needle from the right midaxillary line to enter a hepatic vein. Pressure measurement and CM injection ensure that the position of the needle or the catheter is correct. Thrombosis of the portal vein is an absolute contraindication, which is why indirect splenoportography must be carried out prior to percutaneous hepatophlebography. Serious complications occur in 1.5–4.0% of cases.

4 Cholangiography

Visualization of the bile ducts can be accomplished indirectly or by means of various direct methods. (s. tab. 8.8)

Indirect cholangiography
1. Intravenous injection
2. Intravenous infusion
3. Spiral CT
4. MRI cholangiography
Direct cholangiography
1. Endoscopic retrograde
2. Percutaneous transhepatic
3. Transvenous
4. Intraoperative
5. Postoperative via drain

Tab. 8.8: Indirect and direct methods of cholangiography

4.1 Indirect cholangiography

In terms of the success rate, conventional X-ray diagnosis of the efferent bile ducts cannot be entirely replaced by (stress-free, easy-to-repeat, technically uncomplicated and less costly) ultrasonography. For example, for diagnosing choledocholithiasis, *i.v. cholangiography* and *tomography* are much more efficient (90–92%) than sonography (67%). The use of (invasive) ERC, however, provides three to four times more reliable diagnostic information than does i.v. cholangiography (V. Myllylä et al., 1984). Furthermore, ultrasonography or i.v. cholangiography (as a rule in conjunction with tomography or MRCP) produces a noninvasive, but inadequate assessment of the intrahepatic bile ducts. In this respect, the methods of direct cholangiography are infinitely superior. • The use of i.v. cholangiography is restricted due to severe damage to the liver cells (GPT, GOT > 150 U/l), increased serum bilirubin (> 3 mg/dl) or cholestasis (AP > 300 U/l). It is further limited by the high technical requirements in individual cases (tomography, infusion cholangiography). • In the case of significant sonographic findings in the area of the bifurcation of the cystic duct and common bile duct (e.g. suspected *Mirizzi syndrome*), consideration should first be given to i.v. cholangiography (with tomography) and then to ERC. Intravenous cholangiography is also indicated for noncongested bile ducts and in cases where ERC has proved unsuccessful. (164, 178)

4.1.2 Spiral CT and MRCP

Biliary secretion of CM under **spiral CT** is used to produce 3D models of the biliary tract, enabling 70–75% of intraductal concrements to be detected. Malignant and benign processes were diagnosed in 75% and 93% of cases. (182) In cholestasis, the biliary tract could also be visualized without the use of CM. (190)

The introduction of **MR cholangiography** by B.K. Wallner et al. (1991) represents a significant development in this field. (187) If CM is not used, the biliary passages in the biliary tract are visualized by distinct T_2-weighted sequences in a coronary display. More rapid gradient systems have further improved display quality (161, 180); here it was possible to achieve comparable results to those obtained in MRC and ERC. (159, 169, 181, 186)

4.2 Direct cholangiography

The use of direct cholangiography is indicated (*1.*) if alterations in the area of the efferent bile ducts could not be clarified by ultrasound and i.v. cholangiography or (*2.*) if the use of i.v. cholangiography is contraindicated, not indicated or likely to be inadequate. Various direct cholangiographic methods are available depending on individual pathological situations and diagnostic issues. (188) (s. tab. 8.8)

4.2.1 ERC

► First described by W.S. McCune et al. (1968) and I. Oi et al. (1969), endoscopic retrograde cholangiography (ERC) is now a valuable and standardized examination method.

Indications: Due to the continuous improvement of ERC (better diagnostic value and reduced complication rate), a number of indications have now been established. (s. tab. 8.9)

1. Suspected mechanical obstruction
   - choledocholithiasis
   - bile-duct tumour
   - bile-duct stricture
   - compression of a bile duct, *etc.*
2. Unresolved hepatobiliary diseases
   - primary sclerosing cholangitis
   - chronic (possibly recurrent) cholangitis
   - intrahepatic gallstones
   - parasitic diseases, *etc.*
3. Prior to surgical procedures on bile ducts
4. Postoperative epigastric symptom complex
5. Negative or unresolved cholangiography
6. Suspected bile-duct anomalies, papillomatosis
7. Suspected congenital intrahepatic bile-duct cysts (Caroli's disease)
8. Follow-up biliodigestive anastomosis
9. Suspected acute biliary pancreatitis
10. Contrast-medium intolerance

Tab. 8.9: Indications for endoscopic retrograde cholangiography

1. Endoscopy of the bile duct allows parasitological (e. g. proof of larvae or eggs), bacteriological or cytological *analysis of the bile* in hepatobiliary issues.

2. A number of other new *therapeutic procedures* have developed against the background of ERC, including the transpapillary insertion of stents for palliative bridging of ductal stenosis.

3. In cases of *mechanical jaundice,* not only the location of the obstruction in the biliary tract is determinable, but usually the type and extent of the (partial or complete) obstruction as well. As a result, a decision can often be taken during the same examination concerning causal or palliative treatment. The coagulation parameters should be within a range which renders papillotomy, stone extraction or tissue biopsy possible without danger to the patient. (s. fig. 8.14)

4. The clarification of *hepatobiliary diseases* is an important indication for ERC. (s. tab. 8.9) • Suppurative cholangitis related to mechanical flow obstruction in a bile duct is a clear indication for ERC, whereby appropriate therapeutic measures (e. g. papillotomy, stone extraction, insertion of tubes or stents) should be carried out at the same time. Septic cholangitis is considered to be an emergency indication. • For diagnosing primary sclerosing cholangitis, ERC is the method of choice. Complete visualization of the intrahepatic biliary system ought to be possible with this method.

Success rate: The success rate for visualizing the biliary tract is 95%, whereas in patients with gastric resection (Billroth II) and Braun's anastomosis, the success rate is only 30−40%. Ultrasonography permits the differentiation between intra- and extrahepatic cholestasis in 75−80% of patients, whereas with ERC the rate is 90−95%. For identifying the type of obstruction, ERC shows even better success rates (89% vs. 58%). On the whole, this method provides a definitive diagnosis in biliary tract disorders in 78−93% of cases. (160, 162, 166, 169, 172, 174, 177, 181, 184, 185)

Fig. 8.14: Use of ERC in obstructive jaundice induced by a large biliary concrement, with congested extrahepatic and intrahepatic bile ducts. Secondary findings: shrunken gall bladder with a cholecystocholic fistula

Contraindications: Fundamentally, there are no absolute contraindications to ERC when performed by an experienced endoscopist, except in the case of uncooperative patients. • Clotting disorders, however, call for special caution when applying this method in view of its invasive nature. With organ decompensation, especially cardiac or respiratory insufficiency, or severe arrhythmia, ERC is generally not the primary method for hepatobiliary diagnosis. In cases of oesophageal varices, an intraabdominal increase in pressure due to retching during the examination may promote or cause variceal bleeding. With high-risk patients, antibiotics should be given as a prophylaxis. The patients must be informed of the increased risk associated with the examination.

Complications: Complications include pancreatitis (0.8−1.0%), cholangitis and sepsis (0.6−0.8%), adverse reactions to premedication and contrast media (0.4−0.6%), and instrument-induced injuries (0.2%). The frequency of bacteriaemia is 15%. An increase in pancreatic enzymes is observed in 15−20% of patients, whereas a rise

in transaminases, γ-GT and AP only occurs in isolated cases. Increases in enzymes are mainly found with injections involving high-viscosity CM, larger doses or excessive pressure. • *Sepsis* can develop after injection of CM into a congested biliary tract. Therefore, in this situation, parallel papillotomy and decompression drainage are required together with peri-interventional prophylactic antibiotics. • The complication rate is altogether 1.0−2.3%; the frequency of cardiopulmonary complications in older patients is 8% (166). Lethality is 0.1%.

4.2.2 PTC

► The method of percutaneous transhepatic cholangiography (PTC) was first described by H. Burckhardt et al. in 1921 and by P. Huard et al. in 1937, and revived by R.F. Carter et al. in 1952. Routine use was recommended by F. Glenn et al. in 1962. • After the development of a thin and flexible puncture needle (Y. Tsuchiya, 1969) and using a Chiba needle (K. Okuda et al., 1974), PTC became a widely used clinical method. (174)

Indications: The indications for PTC have become increasingly limited in favour of ERC, since preference is given to the visualization of the biliary tract through the major duodenal papilla (= physiological access) over invasive and non-physiological transhepatic access. Moreover, the rate of complications regarding PTC is clearly higher than with ERC. • *Obstructive jaundice* not clarified by ERC is an indication for diagnostic PTC. However, the higher success rate of approx. 90% for ERC in clarifying obstructive jaundice, compared with approx. 70% for PTC, makes ERC the method of choice. PTC is also indicated if drainage of congested bile is necessary and recommended for preoperative diagnosis or drainage before operations on bile ducts, above all in the area of the hepatic hilus. PTC may also be applied in cases involving nondilated bile ducts where suspected biliary obstruction could not be clarified by i.v. cholangiography and ERC. (s. fig. 8.15) The use of PTC as an operation channel for therapeutic measures in the biliary system is of great importance in a wide range of diseases, e.g. stone extraction, bile-duct dilation, antibiotic rinsing in suppurative cholangitis, electroresection and intraluminal radiation. • With dilated bile ducts, the puncture is successful in >95% and with nondilated bile ducts in 50(−70)% of cases. No more than five attempts at puncture should be made. With a correctly positioned needle in a bile duct, the CM only flows slowly and in a mediocaudal direction, remaining in the vessel once the injection has been stopped. (168, 174, 183, 189)

Technique: PTC is relatively easy to carry out and requires minimal technology. It is performed under sonographic or X-ray control. The target is the liver hilus where it joins with larger bile ducts at the level of the 12th intercostal space, three "finger breadths" from the right margin of the 12th thoracic vertebra. The *target technique of Okuda* has proved useful for determining the correct position and direction of the puncture. (176) • Rapid flow of the CM with a tree-like ramification shows that the needle is located in a branch of the portal vein; some blood escapes from the cannula. Should the CM flow rapidly towards the inferior vena cava, the needle is positioned in a branch of the hepatic vein. Fine and irregular vessels depicted with a slowing down of the mediocaudal flow of the CM suggest a filling of the lymphatic vessels. After administration of the contrast medium and removal of the needle, it is possible, by altering the patient's position, to ensure adequate filling of the intrahepatic bile ducts and gall bladder; when the upper part of the body is raised, the bile duct (= d. choledochus) is also well visualized. One drawback is the general inability to assess the biliary situation distal to the occlusion (comparable with ERC cranial to the occlusion) if this point cannot be visualized due to the fact that the CM was not able to pass the obstruction.

Fig. 8.15: Use of percutaneous transhepatic cholangiography in benign papillary stenosis. Hard fibrotic tissue after repeated passing of gallstones associated with colics over a period of three years. Treatment: papillotomy

Contraindications: Contraindications include clotting disorders, echinococcus cyst, marked ascitis, liver abscess, liver metastases and cirrhosis.

Complications: In 3−6% of cases, complications occur; compiled statistics showed a frequency of up to 10.2% and 13.2%. In 3.4% of cases, a surgical procedure was required. The main complications are bilious peritonitis, haemorrhage, haemobilia, cholangitis and sepsis. Lethality was 0.06−0.08% − even 0.9%. There is a risk of piercing unidentified abscesses, tumours and metastases along the transhepatic route. The gall bladder must also be circumvented. A long intrahepatic course of the puncture channel is designed to ensure greater safety with regard to biliary leakage. Even in cases of incomplete obstruction, biliary decompression (which can be achieved for example by aspirating bile prior to injecting the CM or by rinsing) is advisable in order to avert

dangerous increases in pressure in the bile ducts. As far as possible, the amount of CM should not exceed 20−40 ml. Prophylactic antibiotics are recommended.

Laparoscopic transhepatic cholangiography (LTC)

This technique, as described by M. Royer in 1952, is a PTC variant. Although it entails fewer complications, the success rate is also reduced, since the length of the intrahepatic puncture channel is only 3 cm. The puncture is performed at a point approx. 3 cm away from the falciform ligament and 5 cm cranial to the edge of the liver, with a puncture angle of 45°.

4.2.3 TVC

Transvenous cholangiography (TVC) was described by W. Hanafee et al. in 1967 as a transjugular form of direct cholangiography. In this procedure, a catheter is introduced through the right jugular vein into a hepatic vein; by transhepatic advancing of the catheter, a bile duct is punctured with an improved Ross needle. This method was modified by R. Günther (1975), who used the right subclavian vein as the site of access. (168) Catheterization through a basilic or cubital vein (I. F. Hawkins jr. et al., 1976) is not considered to be of any advantage. TVC is more complicated than PTC in terms of time and instruments. The success rate for congested bile ducts is 65−93% for cases of non-congestion 10−69%. There is no need to prepare for surgery. TVC is only indicated in exceptional cases. • The *complication rate* is 8.9% (mild complications 5.5%, serious incidents 3.4%), with a lethality of 0.4%. The main complications are intraperitoneal bleeding, subcapsular liver haematoma, haemobilia, bilihaemia and sepsis. No bile peritonitis has been reported so far. • *Contraindications* include acute cholangitis, hepatic echinococcus and liver abscess.

4.2.4 PTCS

Percutaneous transhepatic cholangioscopy (PTCS) is indicated (*1*.) to clarify the benignancy or malignancy of bile-duct stenoses, (*2*.) to visualize the biliary tract by X-ray using a guide wire and a catheter positioned by the endoscopist's naked eye, and (*3*.) to perform lithiotripsy of bile duct stones and remove any local obstruction of bile flow. The examination is carried out with a percutaneously placed biliocutaneous fistula, which is stable enough after eight to ten days to permit insertion of a cholangioscope. Endoscopic evaluation is carried out under continuous rinsing with a physiological NaCl solution. (173)

4.2.5 Intraoperative cholangiography

Intraoperative cholangiography was introduced into biliary diagnosis by P. L. Mirizzi in 1932. Since then, this technique has been under development and it is (still) used as an indispensable, additional intraoperative diagnostic tool in borderline cases. Interventions in the area of the gall bladder or bile ducts are generally unacceptable without the possibility of a cholangiographic examination of the biliary tract. (163, 165, 170, 175, 179, 188) • Intraoperative cholangiography should be reserved for resolving special issues. (s. tab. 8.10)

1. Length and width of the common bile duct
2. Choledocholithiasis
3. Hepaticolithiasis
4. Examining the biliary tract for
   - anomalies
   - breaks
   - fistulas
   - stenoses
   - ligatures
   - contour irregularities
   - intraoperative injuries
5. Examining the major duodenal papilla
6. Examining the pancreatic duct, if necessary

Tab. 8.10: Indications for intraoperative cholangiography

Several **methods** are available for intraoperative cholangiography. These are used prior to or after opening the common bile duct: (*1*.) direct cholangiography consisting of puncture of the bile duct by a sharp cannula, (*2*.) cholangiography through the cystic duct, whereby a blunt and curved button cannula or a Nélaton's catheter is inserted by stab incision through the cystic duct (which is situated under the ligatures) into the bile duct, (*3*.) transvesical cholangiography, including the introduction of a special trocar cannula into the fundus of the gall bladder, and (*4*.) cholangiography after choledochotomy by means of a blocker catheter or a double-balloon T-catheter. • Using these methods, the bile ducts can be shown by X-ray in both the direction of the liver and the duodenum. (191)

4.2.6 Postoperative cholangiography

Postoperative cholangiography is an indispensable follow-up prior to removing the drain. This method is aimed at confirming surgical success and obtaining proof of an undisturbed bile flow into the duodenum. The examination, performed with the patient in a head-down position, also enables visualization of the intrahepatic bile ducts, so as to exclude the presence of small residual concrements. The injection of contrast medium can be combined with the simultaneous measuring of pressure. Imaging is performed during consecutive stages of biliary filling.

Synopsis

Since the discovery of X-ray by W. C. Röntgen (1895), several radiological examination methods have been developed. They have also been used in the field of hepatology with great instrumental subtlety and manual skill. These methods have proved irreplaceable in the imaging of vessels and bile ducts. • The development of CT and MRI − in particular helical CT and MRI cholangiography − constitutes a breakthrough in radiology once held to be inconceivable.

► The introduction of various contrast-medium techniques not only in sonography (CEDS) but also in CT and MRI has led to rapid changes in the field of radiological diagnosis in hepatology. • *Particularly in the visualization of portal, venous and arterial vessels, fascinating angiographic tissue reconstruction has become possible, even on an outpatient basis.* • Similarly, with respect to the differentiation of tissue structures, more detailed information, which was long deemed beyond reach, can now be obtained. It is to be expected that even cellular metabolic processes will be shown by imaging techniques in the future − an absolutely fascinating idea!

It was therefore seen as a matter of great importance in this chapter to follow the **path of radiological diagnosis in hepatology**, tracing the course of the examination methods hitherto applied (and now deemed in part to be out of date and obsolete) through to those techniques still undergoing development.

References:

Computer tomography

1. **Alfidi, R.J., Haaga, J., Meaney, T.F., McIntyre, W.J., Gonzalez, L., Tarar, R., Zelch, M.G., Boller, M., Cook, S.A., Jelden, G.:** Computed tomography of the thorax and abdomen; a preliminary report. Radiology 1975; 117: 257−264
2. **Barakos, J.A., Goldberg, H.I., Brown, J.J., Gilbert, T.J.:** Comparison of computed tomography and magnetic resonance imaging in the evaluation of focal hepatic lesions. Gastrointest. Radiol. 1990; 15: 93−101
3. **Bluemke, D.A., Fishman, E.K.:** Spiral CT of the Liver. Amer. J. Roentgenol. 1993; 160: 787−792
4. **Choi, B.I., Lim, J.H., Han, M.C., Lee, D.H., Kim, S.H., Kim, Y.I., Kim, C.:** Biliary cystadenoma and cystadenocarcinoma: CT and sonographic findings. Radiology 1989; 171: 57−61
5. **Choi, B.I., Lee, H.J., Han, J.K., Choi, D.S., Seo, J.B., Han, M.C.:** Detection of hypervascular nodular hepatocellular carcinoma: value of triphasic helical CT compared with iodized-oil CT. Amer. J. Roentgenol. 1997; 168: 219−224
6. **Dillon, E.H., van Leeuwen, M.S., Fernandez, M.A., Mali, W.P.T.M.:** Spiral CT angiography. Amer. J. Roentgenol. 1993; 160: 1273−1278
7. **Dodd, G.D.I., Baron, R.L., Oliver, J.H.I.:** End-stage primary sclerosing cholangitis: CT findings of hepatic morphology in 36 patients. Radiology 1999; 211: 357−362
8. **El-Tahir, M.I., Omojola, M.F., Malatani, T., Al-Saigh, A.H., Ogunbiyi, O.A.:** Hydatid disease of the liver: evaluation of ultrasound and computed tomography. Brit. J. Radiol. 1992; 65: 390−392
9. **Federle, M.P., Blachar, A.:** CT evaluation of the liver: Principles and techniques. Semin. Liver Dis. 2001; 21: 135−145
10. **Freeny, P.C.:** Helical computed tomography of the liver: Techniques, applications and pitfalls. Endoscopy 1997; 29: 515−523
11. **Furuse, J., Maru, Y., Yoshino, M., Mera, K., Sumi, H., Sekiguchi, R., Sataka, M., Hasebe, T., Ochiai, A.:** Assessment of arterial tumor vascularity in small hepatocellular carcinoma. Comparison between color Doppler ultrasonography and radiographic imagings with contrast medium: dynamic CT, angiography, and CT hepatic arteriography. Eur. J. Radiol. 2000; 36: 20−27
12. **Hänninen, E.L., Vogl, T.J., Felfe, R., Pegios, W., Balzer, J., Clauss, W., Felix, R.:** Detection of focal liver lesions at biphasic spiral CT: randomized double-blind study of the effect of iodine concentration in contrast materials. Radiology 2000; 216: 403−409
13. **Halvorsen, R.A., Korobkin, M., Ram, P.C., Thompson, W.M.:** CT appearance of focal fatty infiltration of the liver. Amer. J. Roentgenol. 1982; 139: 277−281
14. **Hodler, J., Meier, P.:** Leberbefall bei Fasciola hepatica: Sonographie und CT. Fortschr. Röntgenstr. 1989; 151: 740−741
15. **Hounsfield, G.N.:** Computerized transverse axial scanning (tomography): Part 1. Description of system. Brit. J. Radiol. 1973; 46: 1016−1022
16. **Inui, A., Fujisawa, T., Suetmitsu, T., Fujikawa, S., Ariizumi, M., Kagimoto, S., Kinoshita, K.:** A case of Caroli's disease with special reference to hepatic CT and US findings. J. Pediatr. Gastroenterol. Nutr. 1992; 14: 463−466
17. **Itai, Y., Araki, T., Ohtomo, K., Kokubo, T., Yoshida, H., Minami, M., Yashiro, N.:** Well-defined dense and continuously spreading enhancement on single level dynamic CT of the liver: a characteristic sign of hepatic cavernous haemangioma. Fortschr. Röntgenstr. 1989; 151: 697−701
18. **Jones, E.C., Chezmar, J.L., Nelson, R.C., Bernardino, M.E.:** The frequency and significance of small ≤ 15 mm) hepatic lesions detected by CT. Amer. J. Roentgenol. 1992; 158: 535−539
19. **Kawamori, Y., Matsui, O., Kitagawa, K., Kadoya, M., Takashima, T., Yamahana, T.:** Macronodular tuberculoma of the liver: CT and MR findings. Amer. J. Roentgenol. 1992; 158: 311−313
20. **Klöppel, R., Reinhardt, M., Lieberenz, S., Fuchs, M., Winnefeld, K., Machnik, G.:** Untersuchungen zur diagnostischen Wertigkeit der CT bei der Siderophilie (primäre idiopathische Hämochromatose). Gastroenterol. J. 1989; 49: 122−125
21. **Levine, C.:** Primary macronodular hepatic tuberculosis: US and CT appearances. Gastrointest. Radiol. 1990; 15: 307−309
22. **Lundstedt, C., Ekberg, H., Hederström, E., Tranberg, K.-G.:** The accuracy of computed tomography of the liver in colo-rectal carcinoma. Clin. Radiol. 1990; 42: 335−339
23. **Lüning, M., Koch, M., Abet, L., Wolff, H., Wenig, B., Buchali, K., Schöpke, W., Schneider, Th., Mühler, A., Rudolph, B.:** Treffsicherheit bildgebender Verfahren (Sonographie, MRT, CT, Angio-CT, Nuklearmedizin) bei der Charakterisierung von Lebertumoren. Fortschr. Röntgenstr. 1991; 154: 398−406
24. **Lüning, M., Simon, C., Dewey, Ch., Decker, T., Sperling, P.:** CT diagnosis of hepatic adenoma. Eur. J. Radiol. 1987; 7: 30−36
25. **Marchal, G., Baert, A.L.:** Dynamic CT of the liver. Radiologe 1992; 32: 211−216
26. **Mathieu, D., Bruneton, J.N., Drouillard, J., Pointreau, C.C., Vasile, N.:** Hepatic adenomas and focal nodular hyperplasia: dynamic CT study. Radiology 1986; 160: 53−58
27. **Mathieu, D., Vasile, N., Menu, Y., van Beers, B., Lorphelin, J.M., Pringot, J.:** Budd-Chiari syndrome: dynamic CT. Radiology 1987; 165: 409−413
28. **Miller, W.J., Federle, M.P., Campbell, W.L.:** Diagnosis and staging of hepatocellular carcinoma: comparison of CT and sonography in 36 liver transplantation patients. Amer. J. Roentgenol. 1991; 157: 303−306
29. **Mortele, K.J., Ros, P.R.:** Imaging of diffuse liver disease. Semin. Liver Dis. 2001; 21: 195−212
30. **Murakami, T., Kim, T., Takamura, M., Hori, M., Takahashi, S., Federle, M.P., Tsuda, K., Osuga, K., Kawata, S., Nakamura, H., Kudo, M.:** Hypervascular hepatocellular carcinoma: detection with double arterial phase multi-detector row helical CT. Radiology 2001; 218: 763−767
31. **Numata, K., Tanaka, K., Kiba, T., Saito, S., Ikeda, M., Hara, K., Tanaka, N., Morimoto, M., Iwase, S., Sekihara, H.:** Contrast-enhanced, wide-brand harmonic gray scale imaging of hepatocellular carcinoma: correlation with helical computed tomographic findings. J. Ultrasound Med. 2001; 20: 89−98
32. **Päivänsalo, M., Lähde, S., Jalovaara, P.:** Computed tomography of hepatic haemangiomas: a chance for a definite diagnosis. Bildgebung 1991; 58: 29−32
33. **Poletti, P.A., Mirvis, S.E., Shanmuganathan, K., Killeen, K.L., Coldwell, D.:** CT criteria for management of blunt liver trauma: correlation with angiographic and surgical findings. Radiology 2000; 216: 418−427
34. **Procacci, C., Fugazzola, C., Cinquino, M., Mangiante, G., Zonta, L., Bergamo Andreis, J.A., Nicoli, N., Pistolesi, G.F.:** Contribution of CT to characterization of focal nodular hyperplasia of the liver. Gastrointest. Radiol. 1992; 17: 63−73
35. **Quinn, St.F., Benjamin, G.G.:** Hepatic cavernous hemangiomas: simple diagnostic sign with dynamic bolus CT. Radiology 1992; 182: 545−548
36. **Raptopoulos, V., Karellas, A., Bernstein, J., Reale, F.R., Constantinou, C., Zawacki, J.K.:** Value of dual-energy CT in differentiating focal fatty infiltration of the liver from low-density masses. Amer. J. Roentgenol. 1991; 157: 721−725
37. **Rogers, J.V., Mack, L.A., Freeny, P.C., Johnson, M.L., Sones, P.J.:** Hepatic focal nodular hyperplasia: angiography, CT, Sonography, and scintigraphy. Amer. J. Roentgenol. 1981; 137: 983−990
38. **Schellinger, D., Di Chiro, G., Axelbaum, S.P., Twigg, H.L., Ledley, R.S.:** Early clinical experience with the ACTA scanner. Radiology 1975; 114: 257−261
39. **Schima, W., Kulinna, C., Ba-Ssalamah, A., Grünberger, T.:** Multidetector computed tomography of the liver. Radiologe 2005; 45: 15−23
40. **Schörner, W., Neumann, K., Langer, M., Heim, T., Keck, H., Felix, R.:** Zur Differentialdiagnostik von Lebermetastasierung und regionaler Leberverfettung: Vergleich von CT und MRT. Fortschr. Röntgenstr. 1991; 154: 628−633
41. **Schweizer, W., Becker, Ch., Tanner, S., Schaeppi, B., Huber, A., Blumgart, L.H.:** Die Bedeutung der Computertomographie (CT) für die konservative Behandlung des Lebertraumas. Schweiz. Med. Wschr. 1993; 123: 577−581
42. **Shamsi, K., De Schepper, A., Degryse, H., Deckers, F.:** Focal nodular hyperplasia of the liver: radiologic findings. Abdom Imaging 1993; 18: 32−38
43. **Shyn, P.B., Goldberg, H.I.:** Abdominal CT following liver transplantation. Gastrointest. Radiol. 1992; 17: 231−236
44. **Sood, G.K., Mahapatra, J.R., Khurana, A., Chaudhry, V., Sarin, S.K., Broor, S.L.:** Caroli disease: computed tomographic diagnosis. Gastrointest. Radiol. 1991; 16: 243−244

45. **Tang-Barton, P., Vas, W., Weissman, J., Salimi, Z., Patel, R., Morris, L.:** Focal fatty liver lesions in alcoholic liver disease: a broadened spectrum of CT appearances. Gastrointest. Radiol. 1985; 10: 133−137
46. **Taylor, C.R.:** Computed tomography in the evaluation of the portal venous system. J. Clin. Gastroenterol. 1992; 14: 167−172
47. **Teefey, S., Baron, R.L., Schulte, S.J., Patten, R.M., Molloy, M.H.:** Patterns of intrahepatic bile duct dilatation at CT: correlation with obstructive disease processes. Radiology 1992; 182: 139−142
48. **Van Thiel, D.H., Hagler, N.G., Schade, R.R., Skolnick, M.L., Pollitt Heyl, A., Rosenblum, E., Gavaler, J.S., Penkrot, R.J.:** In vivo hepatic volume determination using sonography and computed tomography. Validation and a comparison of the two techniques. Gastroenterology 1985; 88: 1812−1817
49. **Vignaux, O., Legmann, P., Coste, J., Hoeffel, C., Bonnin, A.:** Cirrhotic liver enhancement on dual-phase helical CT: comparison with noncirrhotic liver in 146 patients. Amer. J. Roentgenol. 1999; 173: 1193−1197
50. **Vlachos, L., Trakadas, S., Gouliamos, A., Lazarou, S., Mourikis, D., Ioannou, R., Kalovidouris, A., Papavasiliou, C.:** Comparative study between ultrasound, computed tomography, intra-arterial digital subtraction angiography, and magnetic resonance imaging in the differentiation of tumors of the liver. Gastrointest. Radiol. 1990; 15: 102−106
51. **Wan, S.K.H., Cochlin, D.L.:** Sonographic and computed tomographic features of polycystic disease of the liver. Gastrointest. Radiol. 1990; 15: 310−312
52. **Welch, T.J., Sheedy II, P.F., Johnson, C.M., Stephens, D.H., Charboneau, J.W., Brown, M.L., May, G.R., Adson, M.A., McGill, D.B.:** Focal nodular hyperplasia and hepatic adenoma: comparison of angiography, CT, US, and scintigraphy. Radiology 1985; 156: 593−595
53. **Wernecke, K., Rummeny, E., Bongartz, G., Vassallo, P., Kivelitz, D., Wiesmann, W., Peters, P.E., Reers, B., Reiser, M., Pircher, W.:** Detection of hepatic masses in patients with carcinoma: comparative sensitivities of sonography, CT, and MR imaging. Amer. J. Roentgenol. 1991; 157: 731−739
54. **Whitehouse, R.W.:** Computed tomography attenuation measurements for the characterization of hepatic haemangiomas. Brit. J. Radiol. 1991; 64: 1019−1022
55. **Yamashita, Y., Takahashi, M., Kanazawa, S., Charnsangavej, C., Wallace, S.:** Parenchymal changes of the liver in cholangiocarcinoma: CT evaluation. Gastrointest. Radiol. 1992; 17: 161−166
56. **Yates, C.K., Streight, R.A.:** Focal fatty infiltration of the liver simulating metastatic disease. Radiology 1986; 159: 83−84
57. **Zocholl, G., Kuhn, F.-P., Augustin, N., Thelen, M.:** Diagnostische Aussagekraft von Sonographie und Computertomographie bei Lebermetastasen. Fortschr. Röntgenstr. 1988; 148: 8−14

Magnetic resonance imaging

58. **Andersen, P.B., Birgegard, G., Nyman, R., Hemmingsson, A.:** Magnetic resonance imaging in idiopathic hemochromatosis. Eur. J. Haematol. 1991; 47: 174−178
59. **Araki, T., Ohtomo, K., Kachi, K., Monzawa, S., Hihara, T., Ohba, H., Ainoda, T., Kumagai, H., Uchiyama, G.:** Magnetic resonance imaging of macroscopic intrahepatic portal-hepatic venous shunts. Gastrointest. Radiol. 1991; 16: 221−224
60. **Arita, T., Matsunaga, N., Kobayashi, H.:** Budd-Chiari syndrome: peripheral abnormal intensity of the liver on magnetic resonance imaging. Clin. Radiol. 2000; 55: 640−642
61. **Barakos, J.A., Goldberg, H.I., Brown, J.J., Gilbert, T.J.:** Comparison of computed tomography and magnetic resonance imaging in the evaluation of focal hepatic lesions. Gastrointest. Radiol. 1990; 15: 93−101
62. **Ba-Ssalamah, A., Happel, B., Kettenbach, J., Dirisamer, A., Wrba, F., Längle, F., Schima, W.:** MRI of the liver. Clinical significance of nonspecific and liver specific MRI contrast agents. Radiologe 2004; 44: 1170−1184
63. **Birnbaum, B.A., Noz, M.E., Chapnick, J., Sanger, J.J., Megibow, A.J., Maguire, G.Q. jr., Weinreb, J.C., Kaminer, E.M., Kramer, E.L.:** Hepatic hemangiomas: diagnosis with fusion of MR, CT, and Tc-99m-labeled red blood cell SPECT images. Radiology 1991; 181: 469−474
64. **Bonkovsky, H.L., Rubin, R.B., Cable, E.E., Davidoff, A., Rijcken, T.H.P., Stark, D.D.:** Hepatic iron concentration: noninvasive estimation by means of MR imaging techniques. Radiology 1999; 212: 227−234
65. **Butch, R.J., Stark, D., Malt, R.A.:** Magnetic resonance imaging of hepatic focal nodular hyperplasia. J. Comput. Assist. Tomogr. 1986; 10: 874−877
66. **Caudana, R., Morasna, G., Pirovano, G.P.:** Focal malignant hepatic lesions: MR imaging enhanced with gadolinium benzyloxy-propionictetra-acetate (BOPTA) − preliminary results of phase II clinical application. Radiology 1996; 199: 513−520
67. **Coombs, R.J., Woldenberg, L.S., Skeel, R.T., Bishara, H.M., Merrick, H.W.:** Magnetic resonance imaging of hepatic adenoma. Clin. Imag. 1990; 14: 44−47
68. **Dalla Palma, L., Pozzi-Mucelli, R.S.:** Computed tomography and magnetic resonance imaging in diagnosing hepatocellular carcinoma. Ital. J. Gastroenterol. 1992; 24: 87−91
69. **Davolio Marani, S.A., Canossi, G.C., Nicoli, F.A., Alberti, G.P., Monni, S.G., Casolo, P.M.:** Hydatid disease: MR imaging study. Radiology 1990; 175: 701−706
70. **Demas, B.E., Hricak, H., Goldberg, H.I., Margulis, A.R.:** Magnetic resonance imaging diagnosis of hepatic metastasis in the presence of negative CT studies. J. Clin. Gastroenterol. 1985; 7: 553−560
71. **Duewell, S., Marincek, B., Schulthess, von, G.K., Ammann, R.:** MRT und CT bei alveolärer Echinokokkose der Leber. Fortschr. Röntgenstr. 1990; 152: 441−445
72. **Fretz, C.J., Stark, D.D., Metz, C.E., Elizondo, G.,Weissleder, R., Jong-Her Shen, Wittenberg, J., Simeone, J., Ferrucci, J.T.:** Detection of hepatic metastases: comparison of contrast-enhanced CT, unenhanced MR imaging, and iron oxide-enhanced MR imaging. Amer. J. Roentgenol. 1990; 155: 763−770
73. **Fulcher, A.S., Turner, M.A., Franklin, K.J.:** Primary sclerosing cholangitis: evaluation with MR cholangiography−a case-control study. Radiology 2000; 215: 71−80
74. **Gabata, T., Matsui, O., Kadoya, M., Takashima, T., Ueda, Y., Komatsu, Y., Sasaki, M.:** MR imaging of hepatic adenoma. Amer. J. Roentgenol. 1990; 155: 1009−1011
75. **Gillams, A.R., Lees, W.R.:** Recent development in biliary tract imaging. Gastrointest. Endosc. Clin. N. Amer. 1996; 6: 1−15
76. **Goldberg, M.A., Saini, S., Hahn, P.F., Egglin, T.K., Mueller, P.R.:** Differentiation between hemangiomas and metastases of the liver with ultrafast MR imaging: preliminary results with T_2 calculations. Amer. J. Roentgenol. 1991; 157; 727−730
77. **Hamrick-Turner, J., Abbitt, P.L., Ros, P.R.:** Intrahepatic cholangiocarcinoma: MR appearance. Amer. J. Roentgenol. 1992; 158: 77−79
78. **Hayes, A.M., Jaramillo, D., Levy, H.L., Knisely, A.S.:** Neonatal hemochromatosis: diagnosis with MR imaging. Amer. J. Roentgenol. 1992; 159: 623−625
79. **Herborn, C.U., Narin, B., Ruehm, S.G.:** Schistosomia mansoni in the liver. Magnetic resonance images. Röfo. 2002; 174: 495−496
80. **Hirai, K., Aoki, Y., Majima, Y., Abe, H., Nakashima, O., Kojiro, M., Tanikawa, K.:** Magnetic resonance imaging of small hepatocellular carcinoma. Amer. J. Gastroenterol. 1991; 86: 205−209
81. **Honda, H., Onitsuka, H., Murakami, J., Kaneko, K., Murayama, S., Adachi, E., Kanematsu, T., Sugimachi, K., Masuda, K.:** Characteristic findings of hepatocellular carcinoma: an evaluation with comparative study of US, CT, and MRI. Gastrointest. Radiol. 1992; 17: 245−249
82. **Irie, H., Honda, H., Tajima, T., Kuroiwa, T., Yoshimitsu, K., Makisumi, K., Masuda, K.:** Optimal MR cholangiopancreatographic sequence and its clinical application. Radiology 1998; 206: 379−387
83. **Itai, Y., Ohtomo, K., Furui, S., Yamauchi, T., Minami, M., Yashiro, N.:** Noninvasive diagnosis of small cavernous hemangiomas of the liver: advantage of MRI. Amer. J. Roentgenol. 1985; 145: 1195−1199
84. **Ito, K., Mitchell, D.G., Matsunaga, N.:** MR imaging of the liver: techniques and clinical applications. Eur. J. Radiol. 1999; 32: 2−14
85. **Ito, K., Mitchell, D.G., Gabata, T., Hann, H.-W.L., Kim, P.N., Fujita, T., Awaya, H., Honjo, K., Matsunaga, N.:** Hepatocellular carcinoma: association with increased iron deposition in the cirrhotic liver at MR imaging. Radiology 1999; 212: 235−240
86. **Ito, K., Mitchell, D.G., Gabata, T.:** Enlargement of hilar periportal space: a sign of early cirrhosis at MR imaging. J. Magn. Reson. Imag. 2000; 11: 136−140
87. **Itoh, K., Saini, S., Hahn, P.F., Imam, N., Ferrucci, J.T.:** Differentiation between small hepatic hemangiomas and metastases on MR images: importance of size-specific quantitative criteria. Amer. J. Roentgenol. 1990; 155: 61−66
88. **Jansen, T.L.T.A., de Vries, R.A., Kesselring, F.O.H.W., Meijer, J.W.R.:** Magnetic resonance imaging in the staging of hepatic veno-occlusive disease. Eur. J. Gastroenterol. Hepatol. 1994; 6: 453−456
89. **Johnson, C.D.:** Magnetic resonance imaging of the liver: current clinical applications. Mayo Clin. Proceed. 1993; 68: 147−156
90. **Kadoya, M., Matsui, O., Takashima, T., Nonomura, A.:** Hepatocellular carcinoma: correlation of MR imaging and histopathologic findings. Radiology 1992; 183: 819−825
91. **Kim, M.J., Mitchell, D.G., Ito, K., Hann, H.W.L., Park, Y.N., Kim, P.N.:** Hepatic iron deposition on MR imaging in patients with chronic liver disease: correlation with serial serum ferritin concentration. Abdom. Imag. 2001; 26: 149−156
92. **Kim, M.-J., Mitchell, D.G., Ito, K.:** Portosystemic collaterals of the upper abdomen: review of anatomy and demonstration on MR imaging. Abdom. Imag. 2000; 25: 462−470
93. **Koslow, S.A., Davis, P.L., DeMarino, G.B., Peel, R.L., Baron, R.L., van Thiel, D.H.:** Hyperintensive cirrhotic nodules on MRI. Gastrointest. Radiol. 1991; 16: 339−341
94. **Kreeftenberg, H.G. jr., Mooyart, E.L., Huizenga, J.R., Sluiter, W.S., Kreeftenberg, H.G.:** Quantification of liver iron concentration with magnetic resonance imaging by combining T1-, T2-weighted spin echo sequences and a gradient echo sequence. Neth. J. Med. 2000; 56: 133−137
95. **Kreft, B., Steudel, A., Harder, T., Bockisch, A., Jakschik, J.:** Qualitative und quantitative kernspintomographische Befunde der fokal nodulären Hyperplasie der Leber. Fortschr. Röntgenstr. 1990; 152: 649−653
96. **Krinsky, G.A., Lee, V.S., Theise, N.D., Weinreb, J.C., Rofsky, N.M., Diflo, T., Teperman, L.W.:** Hepatocellular carcinoma and dysplastic nodules in patients with cirrhosis: prospective diagnosis with MR imaging and explantation correlation. Radiology 2001; 219: 445−454
97. **Laing, A.D.P., Gibson, R.N.:** MRI of the liver. J. Magn. Reson. Imag. 1998; 8: 337−345
98. **Lalonde, L., Beers, van, B., Jamart, J., Pringot, J.:** Capsule and mosaic pattern of hepatocellular carcinoma: correlation between CT and MR imaging. Gastrointest. Radiol. 1992; 17: 241−244
99. **Lavelle, M.T., Lee, V.S., Rofsky, N.M., Krinsky, G.A., Weinreb, J.C.:** Dynamic contrast-enhanced three-dimensional MR imaging of liver

parenchyma: source images and angiographic reconstructions to define hepatic arterial anatomy. Radiology 2001; 218: 389−394
100. **Lee, M.J., Saini, S., Hamm, B., Taupitz, M., Hahn, P.F., Seneterre, E., Ferrucci, J.T.:** Focal nodular hyperplasia of the liver: MR findings in 35 proved cases. Amer. J. Roentgenol. 1991; 156: 317−320
101. **Lombardo, D.M., Baker, M.E., Spritzer, C.E., Blinder, R., Meyers, W., Herfkens, R.J.:** Hepatic hemangiomas vs metastases: MR differentiation at 1,5 T. Amer. J. Roentgenol. 1990; 155: 55−59
102. **Mahfouz, A.-E., Hamm, B., Taupitz, M., Wolf, K.-J.:** Hypervascular liver lesions: differentiation of focal nodular hyperplasia from malignant tumors with dynamic gadolinum-enhanced MR imaging. Radiology 1993; 186: 133−138
103. **Mahfouz, A.-E., Hamm, B., Taupitz, M.:** Hepatic magnetic resonance imaging: new techniques and contrast agents. Endoscopy 1997; 29: 504−514
104. **Marti-Bonmati, L., Ferrer, D., Menor, F., Galant, J.:** Hepatic mesenchymal sarcoma: MRI findings. Abdom. Imag. 1993; 18: 176−179
105. **Maves, C.K., Caron, K.H., Bisset, G.S., Agarwal, R.:** Splenic and hepatic peliosis: MR findings. Amer. J. Roentgenol. 1992; 158: 75−76
106. **Mueller, G.C., Hussain, H.K., Carlos, R.C., Nieghiem, H.V., Francis, I.R.:** Effectiveness of MR imaging in characterizing small hepatic lesions: Routine versus expert interpretation. Amer. J. Roentgenol. 2003; 180: 673−680
107. **Murakami, T., Kuroda, C., Marukawa, T., Harada, K., Wakasa, K., Sakurai, M., Monden, M., Kasahara, A., Kawata, S., Kozuka, T.:** Regenerating nodules in hepatic cirrhosis: MR findings with pathologic correlation. Amer. J. Roentgenol. 1990; 155: 1227−1231
108. **Noohe, T.C., Semelka, R.C., Woosley, J.T., Pisano, E.D.:** Ultrasound and MR findings in acute Budd-Chiari syndrome with histopathologic correlation. J. Comput. Assist. Tomogr. 1996; 20: 819−822
109. **Ohtomo, K., Araki, T., Itai, Y., Monzawa, S., Ohba, H., Nogata, Y., Hihara, T., Koizumi, K., Uchiyama, G.:** MR imaging of malignant mesenchymal tumors of the liver. Gastrointest. Radiol. 1992; 17: 58−62
110. **Petersein, J., Dewey, Ch., Lüning, M., Schnackenburg, B., Wenig, B., Koch, M., Schneider, T., Mühler, A.:** Quantitative Auswertung der dynamischen MRT mit Gd-DTPA: Vergleich von Hämangiomen und fokalen nodulären Hyperplasien der Leber. Radiolog. Diagnost. 1992; 33: 95−100
111. **Rafal, R.B., Jennis, R., Kosovsky, P.A., Markisz, J.A.:** MRI of primary amyloidosis. Gastrointest. Radiol. 1990; 15: 199−201
112. **Rofsky, N.M., Weinreb, J.C., Bernardino, M.E., Young, S.W., Lee, J.K.T., Noz, M.E.:** Hepatocellular tumors: characterization with Mn-DPDP-enhanced MR imaging. Radiology 1993; 188: 53−59
113. **Siegelman, E.S., Mitchell, D.G., Outwater, E., Munoz, S.J., Rubin, R.:** Idiopathic hemochromatosis: MR imaging findings in cirrhotic and precirrhotic patients. Radiology 1993; 188: 637−641
114. **Stark, D.D., Felder, R.C., Wittenberg, J., Saini, S., Butch, R.J., White, M.E., Edelman, R.R.:** Magnetic resonance imaging of cavernous hemangioma of the liver: tissue specific characterization. Amer. J. Roentgenol. 1985; 145: 213−222
115. **Taylor, C.R., McCauley, T.R.:** Magnetic resonance imaging in the evaluation of the portal venous system. J. Clin. Gastroenterol. 1992; 14: 268−273
116. **Tung, G.A., Vaccaro, J.P., Cronan, J.J., Rogg, J.M.:** Cavernous hemangioma of the liver: pathologic correlation with high-field MR imaging. Amer. J. Roentgenol. 1994; 162: 1113−1117
117. **Vassiliades, V.G., Foley, W.D., Alarcon, J., Lawson, T., Erickson, S., Kneeland, J.B., Steinberg, H.V., Bernardino, M.E.:** Hepatic metastases: CT versus MR imaging at 1,5 T. Gastrointest. Radiol. 1991; 16: 159−163
118. **Vilgrain, V., Fléjou, J.-F., Arrivé, L., Belghiti, J.,Najmark, D., Menu, Y., Zins, M., Vullierme, M.-P., Nahum, H.:** Focal nodular hyperplasia of the liver: MR imaging and pathologic correlation in 37 patients. Radiology 1992; 184: 699−703
119. **Vlachos, L., Gouliamos, A., Kalovidouris, A., Trakadas, S., Lygidakis, N., Matsaidonis, D., Papadopoulos, A., Papavasiliou, C.:** Differential diagnosis of space-occupying lesions of the liver with MR imaging. Hepato-Gastroenterol. 1992; 39: 461−465
120. **Vogl, T.J., Hammerstingl, R., Schnell, B., Eibl-Eibesfeldt, B., Peqios, W., Lissner, J.:** Magnet-Resonanz-Tomographie des hepatobiliären Systems: Indikation, Limitationen und Ausblick. Bildgebung 1992; 59: 195−199
121. **Wenzel, J.S., Donohoe, A., Ford, K.L., Glastad, K., Watkins, D., Molmenti, E.:** Primary biliary cirrhosis: MR imaging findings and description of MR imaging periportal halo sign. Amer. J. Roentgenol. 2001; 176: 885−889
122. **Zech, C.J., Schoenberg, S.O., Herrmann, K.A., Dietrich, O., Menzel, M.I., Lanz, T., Wallnöfer, A., Helmberger, T., Reiser, M.F.:** Modern visualization of the liver with MRI. Current trends and future perspectives. Radiologe 2004; 44: 1160−1169

Angiography

123. **Aspestrand, F., Kolmannskog, F.:** CT and angiography in chronic liver disease. Acta Radiol. 1992; 33: 251−254
124. **Blumke, D.A., Fishman, E.K.:** Spiral CT arterial portography of the liver. Radiology 1993; 186: 576−579
125. **Cavaluzzi, J.A., Sheff, R., Harrington, D.P., Kaufmann, St.L., Barth, K., Maddrey, W.C., White, R.I.jr.:** Hepatic venography and wedge hepatic vein pressure measurements in diffuse liver disease. Amer. J. Roentgenol. 1977; 129: 441−446
126. **Düx, A., Bücheler, E., Thurn, P.:** Die indirekte Splenoportographie: Methodik, Indikationen und Ergebnisse. Fortschr. Röntgenstr. 1967; 106: 183−197
127. **Finucci, G., Bellon, S., Merkel, C., Mormino, P., Tirelli, M., Gatta, A., Zuin, R.:** Evaluation of splanchnic angiography as a prognostic index of survival in patients with cirrhosis. Scand. J. Gastroenterol. 1991; 26: 951−960
128. **Foley, W.D., Stewart, E.T., Milbrath, J.R., San Dretto, M., Milde, M.:** Digital subtraction angiography of the portal venous system. Amer. J. Roentgenol. 1983; 140: 497−499
129. **Freeny, P.C., Vimont, T.R., Barnett, D.C.:** Cavernous hemangioma of the liver: ultrasonography, arteriography, and computed tomography. Radiology 1979; 132: 143−148
130. **Garbagnati, F., Spreafico, C., Marchiano, A., Salvetti, M., Segura, C., Piragine, G.:** Staging of hepatocellular carcinoma by ultrasonography, computed tomography, and angiography: the role of CT combined with arterial portography. Gastrointest. Radiol. 1991; 16: 225−228
131. **Goldberg, M.A., Yucel, E.K., Saini, S., Hahn, P.F., Kaufmann, J.A., Cohen, M.S.:** MR angiography of the portal and hepatic venous system: preliminary experience with echoplanar imaging. Amer. J. Roentgenol. 1993; 160: 35−40
132. **Goldstein, H.M., Neiman, H.L., Mena, E., Bookstein, J.J., Appelman, H.D.:** Angiographic findings in benign liver cell tumors. Radiology 1974; 110: 339−343
133. **Goyen, M., Ruehm, St.G., Debatin, J.F.:** Whole-body MR angiography for arterial screening. Med. Klin. 2002; 97: 285−289
134. **Jain, R., Sawhney, S., Sahni, P., Taneja, K., Berry, M.:** CT portography by direct intrasplenic contrast injection: a new technique. Abdom. Imag. 1999; 24: 272−277
135. **Komori, K., Sonoda, T., Ikeda, Y., Kanematu, T., Sugimachi, K.:** Demonstration of hepatic artery aneurysma by subtraction angiography. Amer. J. Gastroenterol. 1991; 86: 1650−1653
136. **Langer, R., Langer, M., Scholz, A., Neuhaus, P., Astinet, F., Ferstl, F.J., Felix, R.:** Stellenwert der Angiographie und radiologischen Intervention vor und nach Lebertransplantation. Fortschr. Röntgenstr. 1991; 155: 416−422
137. **Lindberg, C.G., Lundstedt, C., Stridbeck, H., Tranberg, K.G.:** Accuracy of CT arterial portography of the liver compared with findings at laparotomy. Acta Radiol. 1993; 34: 139−142
138. **Mateev, B., Wirbatz, W., Kiessling, J., Wittbrodt, S., Eichhorn, H.-J.:** Die Katheterisierung der V. portae über die V. umbilicalis (transumbilikale Portohepatographie). Fortschr. Röntgenstr. 1969; 110: 178−191
139. **Merine, D., Takayasu, K., Wakao, F.:** Detection of hepatocellular carcinoma: comparison of CT during arterial portography with CT after intra-arterial injection of iodised oil. Radiology 1990; 175: 707−710
140. **Meves, M., Apitzsch, D.E.:** Die Lebervenenangiographie zum Nachweis von intrahepatischen Tumoren. Fortschr. Röntgenstr. 1976; 125: 247−251
141. **Oberstein, A., Kauczor, H.U., Mildenberger, P., Ibe, M., Teifke, A., Rieker, O., Gerken, G., Thelen, M.:** Triphasic spiral CT scanning in the diagnosis of liver diseases: comparison with CT arteriography and CT arterioportography. Fortschr. Röntgenstr. 1996; 164: 449−456
142. **Okazaki, M., Ono, H., Higashihara, H., Koganemaru, F., Nozaki, Y., Hoashi, T., Kimura, T., Yamasaki, S., Makuuchi, M.:** Angiographic management of massive hemobilia due to iatrogenic trauma. Gastrointest. Radiol. 1991; 16: 205−211
143. **Ono, N., Toyonaga, A., Nishimura, H., Hayabuchi, N., Tanikawa, K.:** Evaluation of magnetic resonance angiography on portosystemic collaterals in cirrhotic patients. Amer. J. Roentgenol. 1997; 92: 1515−1519
144. **Pavone, P., Marsili, L., Albertini Petroni, G., Cardone, G., Cisternino, S., Di Girolamo, M., Passariello, R.:** Arteriography in diagnosing hepatocellular carcinoma. Ital. J. Gastroenterol. 1992; 24: 92−94
145. **Pollard, J.J., Nebesar, R.A., Mattoso, L.F.:** Angiographic diagnosis of benign diseases of the liver. Radiology 1966; 86: 276−283
146. **Schwartz, D.S., Gettner, P.A., Konstantino, M.M., Bartley, C.L., Keller, M.S., Ehrenkranz, R.A., Jacobs, H.C.:** Umbilical venous catherization and the risk of portal vein thrombosis. J. Pediatr. 1997; 131: 760−762
147. **Stiglbauer, R., Barton, P., Jantsch, H., Pichler, W., Schurawitzki, H., Mühlbacher, F.:** Angiographie nach Lebertransplantation. Fortschr. Röntgenstr. 1990; 153: 357−361
148. **Stulberg, H.J., Bierman, H.R.:** Selective hepatic arteriography. Normal anatomy, anatomic variations, and pathological conditions. Radiology 1965; 85: 46−55
149. **Takahashi, K., Saito, K., Tamura, K., Honda, M., Touei, H., Sakai, O., Kawashima, Y., Kuji, T., Ohtani, M., Kawamoto, T., Ohsawa, T.:** Hepatic neoplasms: detection with hepatoportal subtraction angiography − a new technnique of DSA. Radiology 1990; 177: 243−248
150. **Takayasu, K., Shima, Y., Muramatsu, Y., Goto, H., Moriyama, N., Yamada, T., Makukuchi, M., Yamasaki, S., Hasegawa, H., Okazaki, N., Hirohasi, S., Kishi, K.:** Angiography of small hepatocellular carcinomas: analysis of 105 resected tumors. Amer. J. Roentgenol. 1986; 147: 525−529
151. **Tomczak, R., Zeitler, H., Rilinger, N., Pfeifer, T., Häberle, H.J., Leibing, U., Friedrich, J.M.:** Stellenwert der Portangiographie bei der Verlaufskontrolle der lokoregionären Chemotherapie. Fortschr. Röntgenstr. 1992; 157: 552−554
152. **Vosshenrich, R., Fischer, U., Grabbe, E.:** MR angiography in portal hypertension. State of the art. Radiologe 2001; 41: 868−876
153. **Wannagat, L.:** Die laparoskopische Splenoportographie. Klin. Wschr. 1955; 33: 750−758.

154. **Wannagat, L.:** Das intrahepatische Splenoportogramm bei der Hepatitis. Med. Klin. 1962; 57: 853−857
155. **Wannagat, L.:** Splenoportographie und Segmentangiographie der Leber. Dtsch. Ärztebl. 1977; 2279−2286
156. **Welch, T.J., Sheedy II, P.F., Johnson, C.M., Stephens, D.H., Charboneau, J.W., Brown, M.L., May, G.R., Adson, M.A., McGill, D.B.:** Focal nodular hyperplasia and hepatic adenoma: comparison of angiography, CT, US, and scintigraphy. Radiology 1985; 156: 593−595
157. **Zajko, A.B., Bron, K.M., Starzl, Th.E., van Thiel, D.H., Gartner, J.C., Iwatsuki, S., Shaw, B.W.jr., Zitelli, B.J., Malatack, J.J., Urbach, A.H.:** Angiography of liver transplantation patients. Radiology 1985; 157: 305−311
158. **Zhang, L.J., Qi, J., Shen, W.:** 16-slice CT hepatic venography. Abdom. Imag. 2006; 31: 308−314

Cholangiography
159. **Alcaraz, M.J., De la Morena, E.J., Polo, A., Ramos, A., De la Cal, M.A., Mandly, A.G.:** A comparative study of magnetic resonance cholangiography and direct cholangiography. Rev. Espan. Enferm. Digest. 2000; 92: 433−438
160. **Bilbao, M.K., Dotter, C.T., Lee, T.G., Katon, R.M.:** Complications of endoscopic retrograde cholangiopancreatography (ERCP). A study of 10.000 cases. Gastroenterology 1976; 70: 314−320
161. **Bret, P.M., Reinhold, C.:** Magnetic resonance cholangiopancreatography. Endoscopy 1997; 29: 472−486
162. **Carr-Locke, D.L.:** Overview of the role of ERCP in the management of diseases of the biliary tract and the pancreas. Gastrointest. Endosc. 2002; 56: (Suppl.): 157−160
163. **Corlette, M.B. jr., Schatzki, St., Ackroyd, F.:** Operative cholangiography and overlooked stones. Arch. Surg. 1978; 113: 729−734
164. **Dawson, P., Adam, A., Benjamin, I.S.:** Intravenous cholangiography revisited. Clin. Radiol. 1993; 47: 223−225
165. **Famos, M., Stadler, P., Schneekloth, G.:** Die selektive intraoperative Cholangiographie. Helv. Chir. Acta 1989; 56: 897−901
166. **Fisher, L., Fisher, A., Thomson, A.:** Cardiopulmonary complications of ERCP in older patients. Gastrointest. Endosc. 2006; 63: 948−955
167. **Flamm, C.R., Mark, D.H., Aronson, N.:** Evidence-based review of ERCP: introduction and description of systematic review methods. Gastrointest. Endosc. 2002; 56 (Suppl.): 161−164
168. **Günther, R., Georgi, M., Schaeffer, H.J.:** Transvenöse Cholangiographie und perkutane transhepatische Feinnadelcholangiographie. Dtsch. Med. Wschr. 1980; 105: 255−262
169. **Hintze, R.E., Adler, A., Veltzke, W., Abou-Rebyeh, H., Hammerstingl, R., Vogl, T., Felix, R.:** Clinical significance of magnetic resonance cholangiopancreatography (MRCP) compared to endoscopic retrograde cholangiopancreatography (ERCP). Endoscopy 1997; 29: 182−187
170. **Kakos, G.S., Tompkins, R.K., Turnipseed, W., Zollinger, R.M.:** Operative cholangiography during routine cholecystectomy. A review of 3012 cases. Arch. Surg. 1972; 104: 484−488
171. **Kiesslich, R., Holfelder, M., Will, D., Hahn, M., Nafe, B., Genitsariotis, R., Daniello, S., Maeurer, M., Jung, M.:** Interventional ERCP in patients with cholestasis. Degree of biliary bacterial colonization and antibiotic resistance. Zsch. Gastroenterol. 2001; 39: 985−992
172. **Kuntz, H.D., May, B.:** Endoskopisch-retrograde Cholangiographie bei primären Lebererkrankungen. Med. Welt 1984; 35: 116−119
173. **Maier, M., Kohler, B., Benz, C., Korber, H., Riemann, J.F.:** Perkutane transhepatische Cholangioskopie (PTCS) − eine wichtige Ergänzung in Diagnose und Therapie von Gallenwegserkrankungen. Z. Gastroenterol. 1995; 33: 435−439
174. **Matzen, P., Malchow-Moller, A., Lejerstofte, J., Stage, P., Juhl, E.:** Endoscopic retrograde cholangiopancreatography and transhepatic cholangiography in patients with suspected obstructive jaundice. A randomized study. Scand. J. Gastroenterol. 1982; 17: 731−735
175. **Merrill, J.R.:** Operative cholangiography by direct puncture of the common bile duct. Surg. Gynec. Obstetr. 1984; 158: 331−334
176. **Okuda, K.:** Thin needle percutaneous transhepatic cholangiography − Historical review. Endoscopy 1980; 12: 2−7
177. **Ponchon, T., Pilleul, F.:** Diagnostic ERCP (review). Endoscopy 2002; 34: 29−42
178. **Rasenack, U., Laubenberger, Th.:** Bedeutung der intravenösen Cholangiographie. Dtsch. Med. Wschr. 1984; 109: 1927−1930
179. **Rolfsmeyer, E.S., Bubrick, M.P., Kollitz, P.R., Onstad, G.R., Hitchcock, C.R.:** The value of operative cholangiography. Surgery 1982; 154: 369−371
180. **Schumacher, K.A., Wallner, B., Weidenmaier, W., Friedrich, J.M.:** Biliäre Obstruktion: MR-Cholangiographie mit einer schnellen Gradientenecho-Sequenz (2D CE-Fast). Fortschr. Röntgenstr. 1991; 155: 332−336
181. **Soto, J.A., Barish, M.A., Yucel, E.K., Siegenberg, D., Ferrucci, J.T., Chuttani, R.:** Magnetic resonance cholangiography: comparison to endoscopic retrograde cholangiopancreatography. Gastroenterology 1996; 110: 589−597
182. **Stockberger, S.M., Sherman, S., Kopecky, K.K.:** Helical CT cholangiography. Abdom. Imaging 1996; 21: 98−104
183. **Teplick, St.K., Flick, P., Brandon, J.C.:** Transhepatic cholangiography in patients with suspected biliary disease and nondilated intrahepatic bile ducts. Gastrointest. Radiol. 1991; 16: 193−197
184. **Topazian, M., Kozarek, R., Stoler, R., Vender, R., Wells, C.K., Feinstein, A.R.:** Clinical utility of endoscopic retrograde cholangiopancreatography. Gastrointest. Endosc. 1997; 46: 393−399
185. **Vilgrain, V., Erlinger, S., Belghiti, J., Degott, C., Menu, Y., Nahum, H.:** Cholangiographic appearance simulating sclerosing cholangitis in metastatic adenocarcinoma of the liver. Gastroenterology 1990; 99: 850−853
186. **Vitellas, K.M., Enns, R.A., Keogan, M.T., Freed, K.S., Spritzer, C.E., Baillie, J., Nelson, R.C.:** Comparison of MR cholangiopancreatographic techniques with contrast-enhanced cholangiography in the evaluation of sclerosing cholangitis. Amer. J. Roentgenol. 2002; 178: 327−334
187. **Wallner, B.K., Schumacher, K.A., Weidenmaier, W., Friedrich, J.M.:** Dilated biliary tract: evaluation with MR cholangiography with a T_2-weighted contrast-enhanced fast sequence. Radiology 1991; 181: 805−808
188. **Wamsteker, E.J.:** Updates in biliary endoscopy. Curr. Opin. Gastroenterol. 2006; 22: 300−304
189. **Zajko, A.B., Bron, K.M., Campbell, W.L., Behal, R., van Thiel, D.H., Starzl, Th.E.:** Percutaneous transhepatic cholangiography and biliary drainage after liver transplantation: a five-year experience. Gastrointest. Radiol. 1987; 12: 137−143
190. **Zeman, R.K., Berman, P.M., Silverman, P.M., Cooper, C., Garra, B.S., Patt, R.H., Ascher, S.M.:** Biliary tract: three-dimensional helical CT without cholangiographic contrast material. Radiology 1995; 196: 865−867
191. **Zimmermann, H.-G.:** Intraoperative Gallenwegsdiagnostik. Chirurg 1981; 52: 440−444